STUDY OF SENSOR PROTEIN EXPRESSSION IN NASOPHARYNGEAL CARCINOMA

By

KALISWARAN A/L PANNIRSELVAM

A dissertation submitted to the Department of Pre-clinical Sciences,

Faculty of Medicine and Health Sciences,

University Tunku Abdul Rahman,

In partial fulfilment of the requirement for the degree of

Master of Medical Science

July 2017

ABSTRACT

STUDY OF SENSOR PROTEIN EXPRESSION IN NASOPHARYNGEAL CARCINOMA

KALISWARAN A/L PANNIRSELVAM

Nasopharyngeal carcinoma (NPC) develops from the epithelial lining of nasopharynx. Prominent tumour infiltrating lymphocytes (TIL) seen in the NPC tumour biopsy suggest possible link to immune response function. Pattern recognition receptors (PRR) sense the highly conserved structures in pathogens to initiate immune response. There are three main families of PRR, namely, toll like receptors (TLR), RIG-like receptors (RLR) and NOD-like receptors (NLR). In addition, there are also independent cytosolic DNA sensors. Immune cells are mainly shown to express PRR as do some somatic cells. Even more intriguing, PRR are reported to be expressed in cancers such as ovarian carcinoma, lung carcinoma, and gastric carcinoma with the implication of promoting tumour development. Identifying selected PRR expression in NPC may provide clues to their function. We selected 15 PRR that are involved in virus recognition and are cancer associated. Selected PRR were screened using end point reverse transcription-PCR (RT-PCR). We detected 11 (out of 15) PRR with aberrant expression in NPC cells compared to non-cancerous nasal epithelial cells. We further analysed 6 (out of 11) for their gene expression using semi quantitative real time (qRT)-PCR and protein analysis (western Blot and immunohistochemistry). In this study, we found RIG-I and DDX41 upregulated in NPC cell lines. Significantly high expression of RIG-I was

identified in CNE2 ($p = 0.00$) with 7.66 ± 2.45 fold and HK1 ($p = 0.00$) with 7.52 ± 1.77 fold. EBV-positive C6661 cell line had significant upregulation in the expression of TLR3 (29.40 ± 1.26) ($p = 0.004$) and TLR4 (167.78 ± 28.2 fold) ($p = 0.00$) compared EBV-negative NPC cells. NLRP3 expression was downregulated in the NPC cell line but had constitutive expression in NP69. Future study on microRNA targeting the downstream signalling pathway molecules will provide insights into the regulation of these PRR and their involvement in NPC pathogenesis.

ACKNOWLEDGEMENT

Firstly, I would like to express my appreciation and sincere gratitude to my advisor Asst. Prof. Dr. Leong Pooi Pooi. You have been an excellent mentor in guiding me during the duration of my research and allowing me to grow as a research scientist. I could not have imagined to have a better advisor for my Master of Science study. I would also like to thank Assoc. Prof. Dr. Gan Seng Chiew, Prof. Swaminathan a/l S. Manickam and Prof. Dr. Choo Kong Bung for your brilliant comments and suggestions. I would especially like to thank all present and past members of UTAR Sungai Long Research Lab who have provided me with help or advice.

I would also like to acknowledge with much appreciation, University Tunku Abdul Rahman for their financial support granted through UTARRF and for providing a comfortable working environment. Thank you also to Dr. Kenny Voon Gah Leong from IMU for providing his guidance when performing western bloting. I would like to express my thank you to Prof. George Tsao from the University of Hong Kong for providing the C6661 NPC cell line, Prof Emeritus, Lin Chin Tarng from National University of Taiwan for providing TW01, TW04, TW06 NPC cell lines and Dr. Yap Lee Fah from University Malaya for providing NP69 cell line. Last but not least, a special thanks to my family and friends especially my parents, for giving me their support, love and encouragement to achieve my goal.

APPROVAL SHEET

This dissertation entitled "STUDY OF SENSOR PROTEIN EXPRESSION IN NASOPHARYNGEAL CARCINOMA" was prepared by KALISWARAN A/L PANNIRSELVAM and submitted as partial fulfillment of the requirements for the degree of Master of medical sciences at Universiti Tunku Abdul Rahman.

Approved by:

_____

(Assistant Prof. Dr. Leong Pooi Pooi) Date:……..
Assistant Professor/ Supervisor
Department of Pre-clinical Sciences
Faculty of Medicine and Health Sciences
Universiti Tunku Abdul Rahman

_____

(Associate Prof. Dr. Gan Seng Chiew) Date:……..
Professor/Co-supervisor
Department of Pre-clinical Sciences
Faculty of Medicine and Health Sciences
Universiti Tunku Abdul Rahman

FACULTY OF MEDICINE AND HEALTH SCIENCES

UNIVERSITI TUNKU ABDUL RAHMAN

Date: July 2017

SUBMISSION OF DESSERTATION

It is hereby certified that KALISWARAN A/L PANNIRSELVAM (ID No: 12UMM07911 has completed this dissertation entitled "STUDY OF SENSOR PROTEIN EXPRESSION IN NASOPHARYNGEAL CARCINOMA" under the supervision of Dr. LEONG POOI POOI from the Department of Pre-clinical Sciences, Faculty of Medicine and Health Sciences, and Dr. GAN SENG CHIEW from the Department of Pre-clinical Sciences, Faculty of Medicine and Health Sciences. .

I understand that the University will upload softcopy of my dissertation in pdf format into UTAR Institutional Repository, which may be made accessible to UTAR community and public.

Yours truly,

_____

(KALISWARAN A/L PANNIRSELVAM)

DECLARATION

I KALISWARAN A/L PANNIRSELVAM hereby declare that the dissertation is based on my original work except for quotations and citations which have been duly acknowledged. I also declare that it has not been previously or concurrently submitted for any other degree at UTAR or other institutions.

_____

(KALISWARAN A/L PANNIRSELVAM)

Date: July 2017

TABLE OF CONTENT

LIST OF TABLES

LIST OF FIGURES

LIST OF ABBREVIATION

AIM2	Absent in melanoma 2
AP-1	Activator protein 1
ASC	Apoptosis associated speck like protein containing a CARD
B2M	Beta-2-Microglobulin
bp	Base pair
CARD	Caspase recruitment domain
CRS	Chronic rhinosinusitis
DAB	3, 3'-diaminobenzidine
DAMP	Damage associated molecular pattern
ddH_2O	Double distilled water
DDX41	DEAD Box Polypeptide 41
DMSO	Dimethyl sulfoxide
dNTP	Deoxynucleotide
DNA	Deoxyribonucleic acid
EBERs	Epstein–Barr virus-encoded small RNAs
EBNA	EBV virus DNA and nuclear antigen
EBV	Epstein - Barr virus
GWAS	Genome wide association study
IHC	Immunohostochemistry
IL	Interleukin
IFI-16	Interferon gamma inducible protein-16
IMRT	Intensity-modulated radiation therapy
IRF	Interferon regulatory factor
KSCC	Keratinizing squamous cell carcinoma
LRR	Leucine rich repeat
LRRFIP1	Leucine rich repeat (in FLII) interacting protein
LMPs	Latent membrane proteins
LPS	Lipopolysaccharide
MAPK	Mitogen –activated protein kinase
MyD88	Myeloid differentiation primary response gene 88
MDA5	Melanoma differentiation-associated gene 5
NF-κB	Nuclear Factor Kappa Beta
NKSCC	Non-keratinizing squamous cell carcinoma
NLRs	NOD-like receptors
NLRC4	NLR family CARD domain-containing protein 4
NLRP3	NOD-Like Receptor Family, Pyrin Domain Containing-3
NPC	Nasopharyngeal carcinoma
PAMP	Pathogen associated molecular pattern
PBS	Phosphate buffered saline
PCR	Polymerase chain reaction
PRRs	Pattern recognition receptor
RIG-I	Retinoic Acid-Inducible Protein 1
RLRs	RIG-like receptors

RNA	Ribonucleic acid
RT-PCR	Reverse transcription- PCR
rpm	Resolution per minute
STAT	Signal transducer and activator
TAE buffer	Tris-Acetate-EDTA buffer
TBS	Tris-buffered saline
TLR	Toll like receptors
TILs	Tumour infiltrating lymphocytes
TRIF	TIR-domain containing adaptor inducing interferon –β
UC	Undifferentiated carcinoma
VCA	Viral capsid antigen
qRT-PCR	Quantitative real time-PCR

CHAPTER 1

INTRODUCTION

Nasopharyngeal carcinoma (NPC) is a cancer arising from the epithelial lining of the area of nasopharynx (Chua et al., 2016). According to the World Health Organization (WHO), NPC can be classified into three categories (based on biological appearance of the cell) namely keratinizing squamous cell carcinoma (KSCC), non-keratinizing squamous cell carcinoma (NKSCC) and undifferentiated carcinoma (UC).

Etiological studies on NPC found unique distributions in NPC cancer incidence among patients around the world. High incidence is reported in the populations of Southern China, South East Asia, Northern Africa and the Artic (Boyle & Lewin 2008). In 2012, 866691 cases were reported worldwide with 50831 deaths (Ferlay et al., 2012). In addition to geological variation, certain ethnic groups such as the Bidayuh from Malaysia and the Chinese from Southern China, Singapore, Taiwan and Malaysia had high age-standardized incidence rate per 100000 population (Devi et al, 2004; Boyle & Lewin, 2008). In Malaysia, NPC is the fourth most common cancer in Malaysia according to Malaysia Cancer Report 2011 (Zainal & Nor Saleha 2011).

Several risk factors have been reported to be associated with pathogenesis including environmental factors (Ren et al. 2010) such as food consumption (e.g alcohol and salted fish), occupational health conditions, genetic susceptibity due to polymorphism and presence of latent infection of Epstein - Barr virus (EBV) in NPC. EBV that is foreign to our body and could cause many disease conditions such as NPC, Burkett's lymphoma and Hodgkin lymphoma remain undetected by our body's anti-viral immune response. The tumour may dampen the tumour immune response by executing various tumour suppressor mechanisms. Massive numbers of tumour infiltrating lymphocytes (TIL) were found in tumour biopsies with no implication of improvement in disease condition (Zhang et al., 2010). The migration of lymphocytes would usually be driven by the event of inflammation.

Pattern recognition receptors (PRR) are initial sensor proteins that detect highly conserved structures from microbial origin called pathogen associated molecular pattern (PAMP) to induce secretion of proinflammatory cytokines (Takeuchi & Akira 2010). There are three main families of PRR namely toll like receptors (TLR), NOD-like receptors (NLR) and RIG-like receptors (RLR) (Lee & Kim, 2007). There are also newly discovered PRR classified as cytosolic DNA sensors (Yang et al., 2010; Keating et al., 2016; Thompson et al., 2011). Immune cells are not the only cells that express PRR as several reports suggested that fibroblast cells and epithelial cells could also have constitutive expression of certain PRR (Lin et al., 2007; Sheyhidin et al., 2011). Aside from this, PRR expression in many cancer cell types has been reported and implicated to play a role in cancer development where tumour

cells by manipulating the PRR downstream signalling molecules, induce production of cytokines that are pro-tumour and were reported to be involved in tumour development (Basith et al., 2012; Cao, 2015).

EBV is well noted as a contributing factor in the pathogenesis of NPC PRR as the immune sensor protein should be able to detect the presence of the virus and initiate anti-viral immune response by secreting type 1 interferon (Li et al., 2015). Currently only a handful of PRR (TLR3 and RIG-I) has been reported to be either associated or expressed in NPC (He et al., 2007; Vérillaud et al., 2012). Therefore, identifying PRR that are possibly aberrantly expressed in NPC cells would determine their role in cancer and their expression in NPC. Expression analysis of PRR could provide clues in identifying new therapeutic targets for the treatment of NPC.

General objective of the study is:

1. To study the expression of selected PRR from TLR family (TLR3, TLR4 and TLR9), RLR family (RIG-I), NLR family (NLRP3) and an independent PRR (DDX41) on a panel of NPC cell lines and a non-cancerous nasal epithelial cell line (NP69).

Specific objectives of the study:

1. To screen for PRR expressed in NPC cells for comparison with PRR in non-cancerous nasal epithelial cells using end point RT-PCR.

2. To verify the expression of selected PRR that are abnormally expressed in NPC cells compared to non-cancerous nasal epithelial cells, using quantitative real time RT-PCR.
3. To analyse protein expression pattern of selected PRR in NPC cells and non-cancerous nasal epithelial cells.

CHAPTER 2

LITERATURE REVIEW

2.1 Nasopharyngeal Carcinoma (NPC)

2.1.1 Epidemiology

Nasopharyngeal carcinoma (NPC) can be characterized by its unique geographic distribution. The disease is an uncommon occurrence in many parts of the world such as the United States of America and Europe but more selectively affects populations in. Southern China, South East Asia, Northern Africa & the Artic (Boyle et al., 2011; M.P, 1997). In Malaysia especially in the region of Sarawak, highest incidences of NPC were reported, where age-standardised rates of NPC were 13.5 and 6.5 among men and women, respectively (Boyle & Lewin, 2008; Devi et al., 2004). Furthermore, NPC was recorded as the fourth highest incidence of cancer overall & third highest incidence of cancer among males in Malaysia (Zainal & Nor Saleha 2011).

2.1.2 Classification

The classification system used by World Health Organization (WHO), has subcategorized NPC (based on biological appearance of cancer cells) into keratinizing squamous cell carcinoma, non-keratinizing squamous cell carcinoma and undifferentiated carcinoma.

The classification system used in NPC is particularly important in clinical management as it provides more comprehensive information on survival and suggests treatment options for NPC patients (Blanchard et al. 2015). A study conducted on NPC patients had shown patients with undifferentiated carcinoma were more likely to survive when compared to the other two subtypes (Ou et al., 2007). Moreover, Keratinizing squamous cell carcinoma had shown the worst prognosis overall in patients from USA (Vazquez et al., 2014). The percentage distribution of the different types of NPC differ by the patient's origin e.g. patients from Taiwan, Hong Kong, and Macao-born Chinese are more likely to have undifferentiated carcinoma while those from USA and non-Hispanic white are more likely to get NPC from the other two subtypes (Marks et al. 1998).

Aside from that, NPC tumours are associated with the presence of massive amounts of tumour infiltrated lymphocytes (TILs) (Zhang et al. 2010). It was also reported that, these tumour infiltrating lymphocytes are non-malignant and mainly are cytotoxic T cells (Zhang et al., 2010). It is noteworthy that, these cytotoxic T cells, which are supposed to exhibit anti-

tumour immunity, are not performing their usual task to eliminate tumour cells but their presence in NPC tumour does not seem to favour positive clinical outcome (Yip et al., 2009). The function of tumour infiltrating lymphocytes in NPC is still open for debate but understanding the factors that may influence their migration towards the NPC tumour site may provide a clue to their function in the pathogenesis of NPC.

2.1.3 Pathogenesis

As we know, the incidence of NPC is high in endemic regions and the disease also affects certain ethnic groups more frequently. Study on pathogenesis of NPC proposed that many factors such as environmental exposure, family history, genetic susceptibility and infection by Epstein-Barr virus (EBV) as the possible causes linked to NPC development (Chang & Adami 2006).

Environmental factors such as the consumption of salted fish that contain volatile nitrosamine among the Southern Chinese people have been highly associated with high risk of NPC (Ning et al., 1990). Tobacco smoking and alcohol have also been linked to risk of NPC found in patient case related studies (Tsai et al., 2016). It was also reported that occupational exposure to wood dust particles, metal, construction sites, chemical in textile industry, smoke particles and other materials were other factors associated with risk of NPC (Armstrong et al. 2000).

Several genetic susceptibility loci had been associated with NPC risk, namely 3p21.31-21.2 (Xiong et al. 2004), 6p21 (Lu et al., 1990) and 5p13 (Hu et al., 2008). Genome wide association study (GWAS) conducted in Chinese population of Southern China identified TNFRSF19 on chromosome 13q12, MDS1-EVI1 on 3q26 and CDKN2A-CDKN2B gene cluster on 9p21 (Bei et al. 2010) to be associated with NPC.

The association between EBV infection (especially at nasal epithelial cells) and NPC is well noted. Patients with NPC often present with elevated IgG and IgA to EBV viral capsid antigen (VCA) and early antigen (EA) (Henle & Henle 1976). Other than that, latent infection of EBV has been identified in all three WHO classified NPC subtypes (Neoplasia et al. 1995). It is well noted that EBV infects almost everyone in the world and has been linked to several malignancies involving lymphoid and epithelial cells such as NPC, Hodgkin disease and gastric carcinoma. EBV infected B-lymphocytes had alteration in growth, when cultured *in vitro,* which resulted in growth transformation and they did not replicate to produce virions during this period (Bornkamm & Hammerschmidt 2001). As far as we know, EBV infection in B-lymphocytes is able to alter the growth *in vitro* resulting in growth transformation (Bornkamm & Hammerschmidt 2001).

Many studies have been conducted to better explain the role of EBV in NPC. Multiple viral genes have been identified to be responsible in the regulation of latent infection of EBV, namely, Latent Membrane Proteins (LMPs) (Frech et al., 1993), EBV nuclear antigens and two non-coding nuclear

RNAs (e.g EBERs) (Kang & Kieff 2015). Frech et al. (1993) reported that the LMP 1 and LMP 2 were presented at elevated levels in NPC. However, LMP1 was only required in B- cell immortalization but not in epithelial cells. LMP1 only induces growth promoting effects and not growth transformation (Young & Rickinson, 2004; Fleming & Paige, 2002). It is still unclear whether EBV has direct involvement in the transformation of nasal epithelial cells. Other possible factors related to EBV and development of NPC are still under investigation. In one study, EBV infected T cells are suggested to be the source of EBV infection in epithelial cells and induced virus replication in epithelial cells (Wen et al, 1997).

2.1.4 Current Management Strategies

Currently the main treatment option for NPC is radiotherapy as NPC is highly radiosensitive (Wei & Kwong, 2010). Radiotherapy is used for all stages of NPC without distant metastases. For instance, the 2 dimensional (2D) radiotherapy has been used to control tumours and the rate of success depends on the severity of the disease. However, this method has come with serious side effects as it may also target tissues that surround the NPC tumour as they are also radiosensitive (Waldron et al. 2016). The 2D radiotherapy limitation was overcome with the introduction of 3D conformal radiotherapy and intensity-modulated radiation therapy (IMRT) (Cheng et al., 2001). IMRT is a more advanced 3D conformal radiotherapy where high dose of radiation can be applied to the tumour and low dose to normal tissues. With that, IMRT is known as the most viable choice for standard NPC care to date. Besides being

radiosensitive, NPC is also chemosensitive (Wei & Kwong, 2010). Chemotherapy is often used in conjunction with radiotherapy to treat NPC with distant metastasis because it is difficult to be treated with radiotherapy alone (Rossi et al. 1988). Intensity modulated radiotherapy can be used concurrently with chemoradiation to provide a more effective treatment in improving the overall condition of NPC patients (Wei & Kwong, 2010).

2.2 Pattern Recognition Receptors

Toll like-receptors (TLR), nucleotide-binding oligomerization domain (NOD)-like receptors (NLR) and retinoic acid-inducible protein gene (RIG) - I like receptor (RLR) are the three reported main families of PRR (Lee & Kim, 2007). Aside from that, there are also some independent newly discovered cytosolic DNA sensor proteins such as LRRFIP1, DDX41, AIM2 and ZDBP-1(Bowie, 2012; Choubey et al., 2000; Osorio et al., 2011). The known expressors of these sensor proteins are the immune cells such as leucocytes, dendritic cells, and macrophages. Some PRR can be found on epithelial cells or fibroblast cells (Lebedev & Ponyakina, 2006; Pandey et al., 2015; Lin et al., 2007).

PRR mainly recognizes pathogen associated molecular pattern (PAMP) to initiate production of proinflammatory cytokines or interferons (Kawai & Akira 2011). PAMP are the structures conserved in the pathogens (Tang et al., 2012). While regulated inflammatory response is beneficial to host, prolonged inflammation can be detrimental to the host because cells in the affected site

are constantly being damaged and repaired with multiple episodes of inflammatory responses with the aim to eliminate foreign threats (Basith et al., 2012). The repeated cycle of cell repair and inflammation that may produce errors and accumulation of these errors such as genetic mutations may eventually lead to cellular malignant transformation resulting in tumour formation (Kutikhin et al., 2011). Therefore, deregulation in PRR may be a contributing factor in cancer development.

The normal functions of PRR are as detectors of the immune system and initiators of an immune response. The receptors and the molecules that are involved in immune response need to be tightly regulated so that once the threat is eliminated, receptor and molecules can return to their normal state. Deregulation in expression of PRR due to mutation or failure to eliminate threat could result in events such as prolonged inflammation which eventually develop into more severe conditions such as cancer (Takeuchi & Akira 2010). The aberrant expression of PRR in malignant cells could manipulate key regulatory molecules involved in inflammation to respond in favour of tumour development by secreting pro-tumour cytokines (Werts et al. 2011).

Despite their function in immune cells and some somatic cells, PRR were also found expressed in many cancer types including oral carcinoma (Ng et al. 2011), ovarian carcinoma (Zhou et al., 2009), lung carcinoma (Zhang et al., 2009), gastric carcinoma (Schmaußer et al., 2005a) as shown in Table 2.1, with implication of their role in cancer development. Pathogen induced TLR signalling that is independent of MyD88 has been implicated to be associated

with inflammation related cancers (Niedzielska et al. 2009) as inflammation induced from persistent infection drives the progression from adenoma to invasive carcinoma. TLR have also been associated with hepatocellular carcinoma with high expression of TLR3, TLR4 and TLR9 in NPC tumour samples (Eiró et al. 2014). On the other hand, TLR expression on gastric carcinoma was shown to allow interaction with *H. pylori*, a pathogen highly associated with gastric cancer, ultimately leading to overproduction of IL-8, a gastric cancer promoting factor (Schmaußer et al., 2005). Overexpression of AIM2 and IFI16 showed possible relation to pathogenesis in oral squamous cell carcinoma through association with NF-κB (Kondo et al. 2012). Given the numerous reports on the expression of PRR in cancer (Table 2.1) and their association with chronic inflammation as well as cancer, it would be interesting to find out the expression of pattern recognition receptors in NPC. Identifying and understanding pattern recognition receptors expression in cancer as opposed to normal epithelial cells may even help the development of these receptors as therapeutic targets (Ridnour et al. 2013).

Table 2.1: Pattern recognition receptor in different cancer types

Cancer type	PRR found
Nasopharyngeal carcinoma	TLR3 (Iwakiri 2014), RIG-I (Duan et al. 2015).
Esophageal squamous cell carcinoma	RIG-I (Kutikhin & Yuzhalin 2012), TLR3, TLR4, TLR7, TLR9 (Sheyhidin et al. 2011).
Gastric cancer	TLR2 (Tye et al. 2012), TLR 4, TLR5, TLR9 (Schmaußer et al. 2005).
Breast cancer	AIM2 (Patsos et al. 2010), TLR4 (Mehmeti et al. 2015).
Lung cancer	TLR4 (He et al. 2007a).
Ovarian cancer	TLR2, TLR3, TLR5 (Zhou et al. 2009), TLR 4 (Kelly et al. 2006).
Colorectal cancer	TLR 4 (Li et al. 2014).

2.2.1 Toll Like Receptors family (TLR)

TLR are type 1 transmembrane proteins (Kawai & Akira 2011). There are ten TLR namely, TLR 1 to 10. These members can function in the recognition of the variety of PAMP (Sandor & Buc 2005). The structure of TLR (Figure 2.1) consists of an extracellular leucine rich repeat (LRR) domain that functions in the recognition of diverse pathogen molecular motifs. On the other hand, intracellular Toll/Interleukin-1 receptor (TIR) domain is able to recruit myeloid differentiation primary response gene 88 (MyD88) and TIR-domain containing adaptor inducing interferon –β (TRIF) upon activation (Kumar et al., 2009).

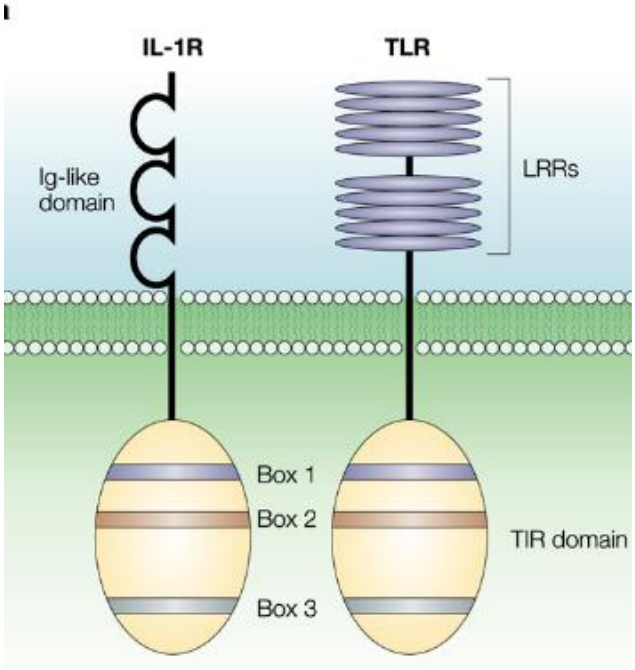

Figure 2.1: Protein structure of TLR. LRR are located in the extracellular matrix while TIR are located in the intracellular compartment of the cells. (Adopted from Akira & Takeda, 2004)

TLR are mainly expressed on the cell surface and are important in recognizing microbial components. Nevertheless, a small group of TLR namely TLR3, TLR7, TLR8 and TLR9 are found in the intracellular compartment where their recognition of ligand occurs (Kawai & Akira 2010). When TLR detects a ligand it would cause the reorientation of the TIR domain (Basith et al., 2011) which serves as activating factor for the recruitment of downstream adapter proteins such as MyD88 and subsequently activation of transcriptional factors such as NF-κB and AP-1, leading to secretion of proinflammatory cytokines. In the MyD88-independant signalling pathway, TIR domain-containing adaptor inducing interferon (IFN)-β (TRIF) is recruited instead of MyD88 (Basith et al. 2012). Activation via TRIF pathway leads to activation of a different transcriptional factor namely IFN-regulatory factor 3

(IRF-3) involved in interferon related function (Kawai & Akira 2005, Basith et al. 2012). The events involved in the intracellular signalling pathway of TLR are further illustrated and summarised in Figure 2.2.

2.2.2 Toll Like Receptor 3 (TLR3)

TLR3 is located at both the surface membrane as well as in the intracellular vesicles (Kawai & Akira 2010). TLR3 detects double stranded (dsRNA) of viral origin (Zhang et al., 2009). Under normal condition, when TLR3 is triggered, it induces production of type 1 interferon (IFN), inflammatory cytokines/chemokines (Xagorari & Chlichlia 2008). TLR3 activates the mitogen –activated protein kinase (MAPK) and TNFR-associated factor (TRAF) for production of inflammatory cytokines such as type 1 interferon (Chiron et al., 2009).

Many studies reported genetic polymorphism in TLR3 with implication of relation to disease conditions such as cancer in patients from Southern China as well as North Africa (He et al., 2007; Moumad et al., 2013). Aside from that, high expression of TLR3 was reported to be associated with cancer development progression in esophageal squamous cell carcinoma, ovarian cancer cell lines and NPC (Sheyhidin et al., 2011; Zhou et al., 2009).

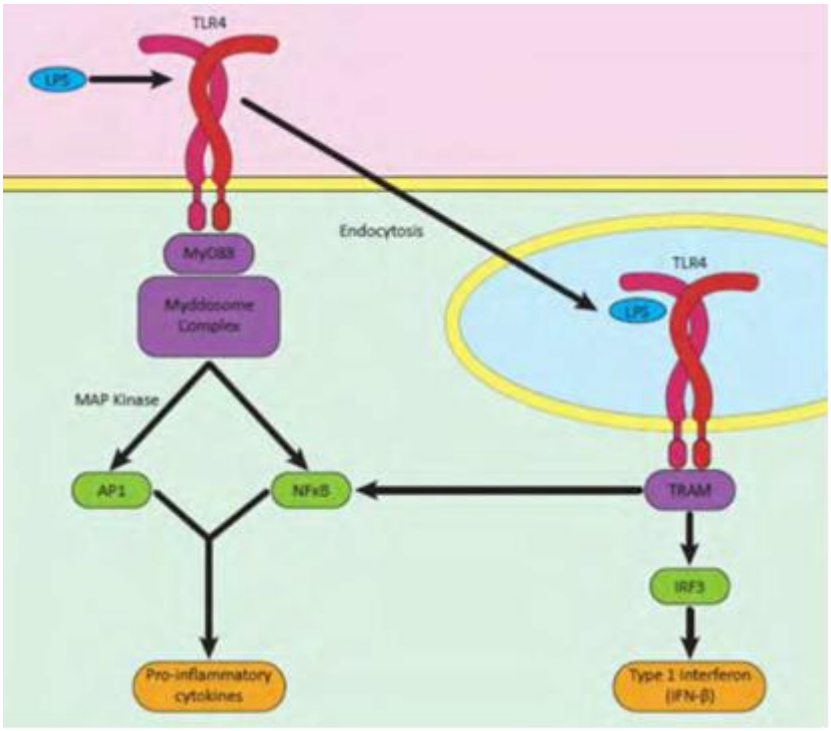

Figure 2.2: Intracellular pathway of activation of TLR. Activation via TRAF adapter protein and subsequently activation of transcriptional factor IRF3 result in production of type 1 interferon while activation via MyD88 adaptor protein caused subsequently activation of transcriptional factor AP-1 and NF-κB, resulting in pro-inflammatory cytokines (Adopted from Jopeace et al., 2012).

2.2.3 Toll Like Receptor 4 (TLR4)

TLR4 detects lipopolysaccharides (LPS) and is primarily found on the cell membrane (Kawai & Akira, 2010). Its adaptor protein MyD88 is recruited to the cell membrane which subsequently activates the interleukin-1 receptor-associated kinase-1 (IRAK-1) and TRAF pathway involving NF-κB to promote the expression of inflammatory cytokines and MAPK pathway and ultimately inducing secretion of interferons (Garc 2007).

High expression of TLR4 has been shown in various disease conditions such as Crohn's disease, and gastric carcinoma (Cario & Podolsky, 2000; Schmaußer et al., 2005). Aside from that, functional TLR4 expression was detected in human lung cancer and capable of inducing the secretion of cytokines that are beneficial in tumour development (He et al., 2007). To further support their pro-tumour activity, human lung cancer was capable of activating NF-κB transcriptional factor when induced by LPS, resulting in apoptosis resistance (He et al., 2007).

2.2.4 Toll Like Receptor 6 (TLR6)

TLR6, a member of TLRs, is localized on the surface membrane and able to detect diacyl lipopeptide (Kawai & Akira 2010). When TLR6 detects a ligand, it recruits adaptor molecule, MyD88, which then triggers a cascade of signalling pathway that ultimately activates NF-κB and interferon regulatory factor (IRF) to produce inflammatory cytokines, chemokines and interferon (Kumar et al. 2009).

Polymorphism in TLR6 could result in deregulation in their function leading to increased susceptibility to pathogen infection in affected cells. Pathogen infections are often the precursor to developing more severe diseases such as complicated skin and skin structure infections and Graves' disease (Xiao et al., 2015; Stappers et al., 2010).

2.2.5 Toll Like Receptor 9 (TLR9)

These receptors are localized mainly on the surface membrane and endosome (Kawai & Akira 2010) and able to detect unmethylated CpG of bacteria and DNA viruses. Upon interaction with the ligands, activated TLR9 leads to translocation of adaptor protein MyD88 to the cell membrane, leads to activation of the interleukin-1 receptor-associated kinase-4 (IRAK-4) and the transcriptional factor interferon regulatory factor-7 (IRF7) resulting in type 1 interferon secretion. Simultaneously, activation of TLR9 is also responsible in inducing the secretion of immune regulatory cytokines that functions in modulating inflammatory responses and one such cytokine is IL-10. Therefore, proper regulation of TLR9 is important to ensure TLR9 functions according to need (Krieg 2006).

Decreased expression of TLR9 was found in disease conditions such as chronic rhinosinusitis (CRS) and this finding was implicated to play a role in the impairment of innate immune response to pathogens (Ramanathan et al. 2007). On a different note, significantly high expression of TLR9 was found in lung cancer specimens compared to tumour free lung tissue and suggested that TLR9 may be involved in the development of the disease (Zhang et al., 2009).

2.2.6 Toll Like Receptor 10 (TLR10)

TLR10 is localized on the surface membrane (Kawai & Akira 2010). TLR10 does not have well-established information on its ligand of detection. However, it was later found that its expression in human macrophages was related to infection by influenza virus (Lee et al., 2014). TLR 10 is the least investigated member of TLR but its ability to sense viral infection and induce antiviral response makes it an interesting target of investigation in NPC as EBV is known to be associated with NPC (Chan et al., 2002).

2.3 Nucleotide-Binding Oligomerization Domain (NOD)-Like Receptors (NLR)

This PRR has a total of 23 NLR identified in humans (Franchi et al., 2010). NLR have an N-terminal protein-binding effector domain (consisting of a caspase activating and recruitment domain (CARD), pyrin domain (PYD) and baculovirus inhibitor of apoptosis repeat (BIR) domain also referred to as acidic domain), NOD or NBD – nucleotide-binding domain (NACHT) and C-terminal leucine rich repeat (LRR).

The centrally located nucleotide-binding and oligomerization (NACHT) domain is important for ligand-induced, ATP-dependent self-oligomerization while C-terminal LRR domain functions to bind to microbial PAMPs or host

damage associated molecular patterns (DAMPs) (Franchi et al. 2010). Members of this family include Nod1, Nod2, and inflammasomes such as NLRC4, NLRP1 and NLRP3 (Franchi et al. 2010).

Under normal conditions, when PAMP or DAMP is detected, the activated NLRP proteins would recruit apoptosis associated speck like protein containing a CARD (ASC) and pro-caspase 1 forming the inflammasome complex as shown in Figure 2.3. The formation of inflammasome complex activates caspase-1 resulting in maturation and secretion of proinflammatory cytokines such as IL-1β and IL-18 cytokines and subsequently inflammation (Werts et al. 2011). The event of NLR protein intracellular signalling pathway is illustrated and summarized in Figure 2.4.

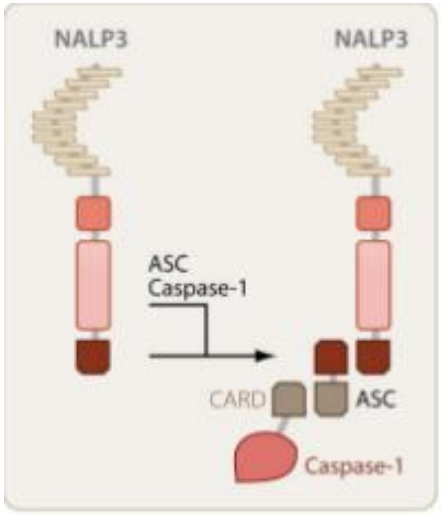

Figure 2.3: The NLRP3 inflammasome complex structure. NLRP3 association with ASC and caspase-1 formed the complex that function in immune response. (Adopted from Martinon et al., 2009).

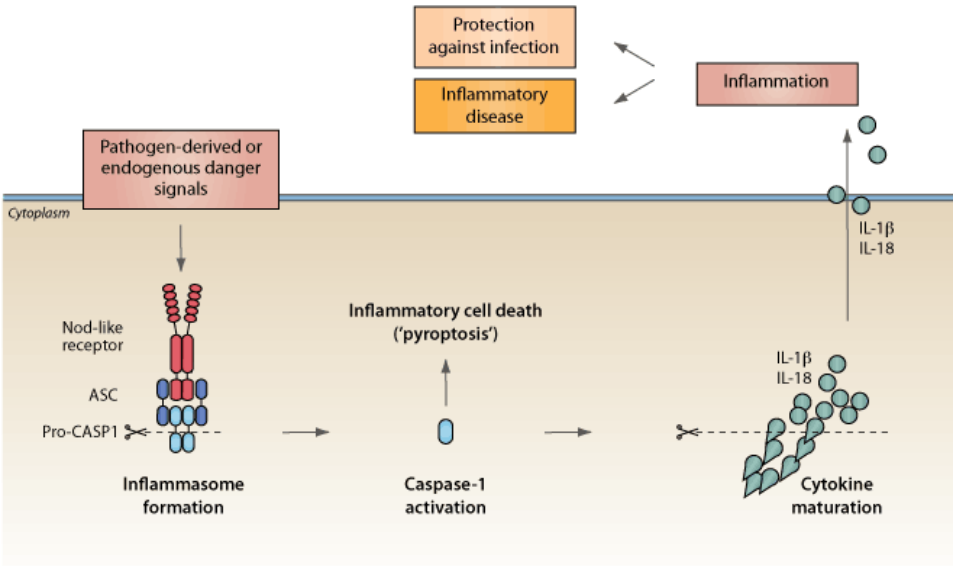

Figure 2.4: Activation of NLR intracellular signalling pathway. PAMP detection recruits ASC containing Pro-caspase 1 and subsequently cleaves caspase 1 to its active form and result in secretion of pro-inflammatory cytokines (Adopted from Tschopp & Schroder, 2010)

2.3.1 NLR family CARD domain-containing protein 4 (NLRC4)

NLRC4 is localized in the cytosol and is responsible for the detection of virulent type pathogens and bacterial flagellin. Inflammasome complex consisting of NLRC4 and ASC containing pro-caspase 1 activates caspase-1 leading to production of inflammatory response in macrophages (Sutterwala et al., 2007; Case & Roy, 2011). Aside from caspase 1, caspase 7 was also found downstream of NLRC4 and their activation leads to host defence against intracellular bacterium infection such as *Legionella pneumophila* infection (Akhter et al. 2009).

Inherited mutation in NLRC4 has been associated with autoinflammation, for example, cold autoinflammatory syndrome (FCAS) (Kitamura et al, 2014). NLRC4 expression may be crucial for tumour immunity; absence of NLRC4 and caspase 1 in mice cells results in enhanced proliferation, reduced apoptosis in colon tumour tissue, and overall enhanced tendency for tumour formation (Hu et al., 2010).

2.3.2 NOD-Like Receptor Family, Pyrin Domain Containing-3 Protein (NLRP3)

NOD-like receptor family, pyrin domain containing-3 protein (NLRP3) is an inflammasome structure (Figure 2.3 B) localized in the cytosol and responsible for the detection of ligands such as microbial components, viral RNA, DAMP and ROS-generating mitochondria. Upon interaction with ligand, NLRP3 inflammsome complex cleaves caspase 1, leading to the production of type 1 interferon (Eicke Latz, 2012; Schroder & Tschopp, 2010; Zhou et al, 2011; Tschopp & Schroder, 2010; Allen et al., 2009).

Previous studies reported that a mutation in NLRP3 gene had resulted in a severe autoinflammation in mice (Chae et al. 2011). Another study found that deregulation in NLRP3 was associated with progression of hepatocellular carcinoma (Wei et al., 2014). On the other hand, the activation of NLRP3 was shown to promote the proliferation and migration of A549 lung cancer and cancer metastasis in gastric cancer (Wang et al., 2016; Xu et al., 2013).

2.4 Retinoic Acid-Inducible Gene (RIG) - I Like Receptor (RLR) and other cytosolic DNA receptors

RLR has two repeats of caspase activation and recruitment domain (CARD), a central H-box RNA helicase/ATPase domain and a C- terminal repressor domain (Onoguchi et al. 2011; Wilkins & Gale, 2010). RLR detects RNA molecules of the pathogens. Members of this family include RIG-I, melanoma differentiation-associated gene 5 (MDA5) (Loo & Gale, 2011). There are also other cytosolic DNA receptors such as DDX41 (Jensen & Thompson, 2012), LRRFIP1 (Keating et al., 2016) and AIM2.

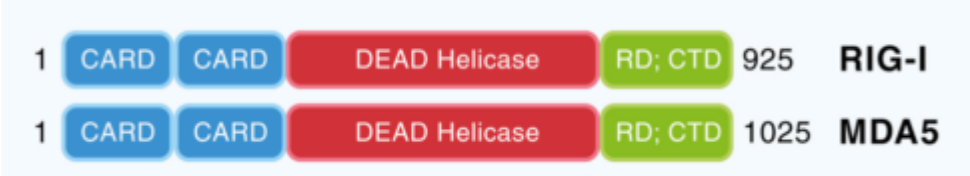

Figure 2.5: Representation of RLR protein structure. The protein structure of RLRs consist of a CARD domain, a central H-box RNA helicase/ATPase domain (DEAD Helicase) and a C- terminal repressor domain (CTD).

When a ligand is detected by RIG-I, the adapter molecule mitochondrial antiviral signalling protein (MAVS) is recruited which then triggers a signalling cascade that activates downstream molecules such as tumour necrosis factor (TNF) receptor-associated factor 3 (TRAF3) and TANK -binding kinase 1 (TBK1) which then activates IFN regulatory factor (IRF) -3 and IRF-7 transcriptional factors which are required for induction of interferons secretion (McCartney & Colonna 2009). Alternatively, signalling via adapter molecule MAVS in association with another signalling molecule, FAS associated death domain (FADD)-containing protein is able to activate

caspase-8 and caspase-10 together with NF-κB resulting in inflammatory response (McCartney & Colonna 2009).

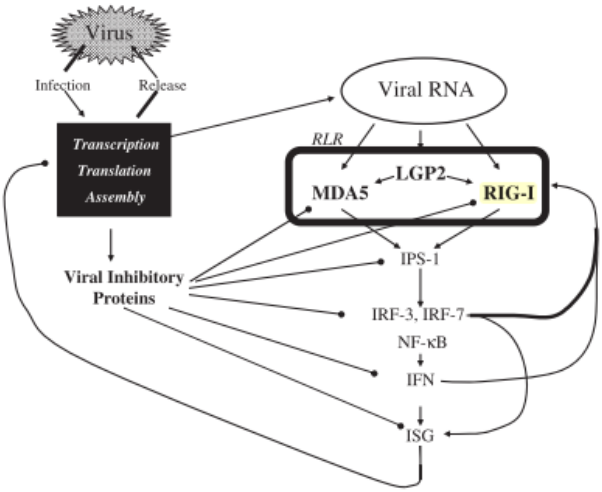

Figure 2.6: RLR intracellular signalling pathway. Viral RNA detected by RLRs and via adapter protein IPS-1and activation of transcriptional factors resulting in secretion of interferon (Adopted from Onoguchi et al., 2011).

2.4.1 Melanoma differentiation-associated gene 5

MDA5, a member of RLR receptor family is located at the cytoplasm and it recognize dsRNA (Langereis et al., 2013). Signalling in MDA5 involves activation of MDA5 leading to recruitment of MAVS which in turn activates IκB kinase epsilon (Iκκ-ε) and TANK-binding kinase 1 (TBK1) complex as well as the IκB kinase beta (Iκκ-β) complex. These kinase complexes would then phosphorylate transcription factors IRF3 and NF-κB, respectively, resulting in the transcription of type 1 interferon (IFN-α/β) genes and other proinflammatory cytokines (Seth et al., 2005).

The mutation discovered in MDA5 was a factor for the autoimmune condition found in the mice (Funabiki et al. 2014). Funabiki et al. (2014) reported that mutation had induced conformational change of the molecule that allows MDA5 to be activated even with absence of viral ligand. MDA5 as a sensor of dsRNA, has the potential to detect Epstein-Barr Virus- encoded small RNA (EBER) thus may have a function to play in EBV related diseases and thus making them a potential candidate for investigation in NPC (Vérillaud et al. 2012).

2.4.2 Retinoic Acid-Inducible Protein I

RIG-I is located in the cytoplasm and it recognizes non-self RNA motif. RIG-I recognizes RNA containing 5'- triphosphate as well as relatively small (< 2.0-kb) double stranded RNA (dsRNA) or base-paired RNA molecules (Langereis et al. 2013). RIG-I receptor shares a similar signalling pathway as MDA5 which results in recruitment of MAVS which in turn activates the Iκκ-ε and TBK1 complexes as well as the Iκκ-β complex. These kinase complexes would then phosphorylate transcription factors IRF3 and NF-κB, respectively, resulting in the transcription of type 1 interferon (IFN-α/β) genes and other proinflammatory cytokines (Seth et al. 2005).

Previous study has shown that EBER from EBV is able to trigger RIG-I expression via NF-κB and IRF3, leading to inflammatory responses (Duan et al. 2016). The study also reported that knockdown of RIG-I resulted in increased tumour burden in mice.

2.4.3 Dead Box Polypeptide 41

Dead Box Polypeptide 41 (DDX41) is located in the cytoplasm and recognizes dsDNA of microbial or viral origin via its DExD/H box domain and interacts with endogenous STING and TBK1, leading to type 1 interferon production in dendritic cells (Broz & Monack, 2013; Zhang et al. 2011; Bowie, 2012),

Other DEAD box proteins are involved also in other processes that are key to cellular proliferation and neoplastic transformation and investigating DDX41 expression in NPC tumour may provide clues to its role in NPC development (Fuller-Pace 2013).

2.4.4 Absence in Melanoma 2

Absence in Melanoma 2 (AIM2) is located in the cytoplasm (Choubey et al., 2000). When expressed in macrophage, it recognizes ligand double stranded DNA (dsDNA). Upon detection of ligand, AIM2 recruits apoptosis-associated speck-like protein (ASC) protein and caspase 1 to form an inflammasome complex. The inflammasome then cleaves procaspase 1 into its active form resulting in inflammatory responses (Jin et al., 2013; Tsuchiya et al., 2010).

AIM2 has been implicated to associate with cancers such as colon cancer and indicated to be responsible for their invasive phenotype by modulating expression of invasion-associated genes such as gene for vimentin and melanoma cell adhesion molecules leading to metastasis (Patsos et al., 2010). The co-expression of AIM2 and interferon inducible 16 (IFI16) have synergistically activated the NF-kB signalling that may have an important role in tumourigenesis of p53- negative oral squamous cell carcinoma (OSCC) (Kondo et al. 2012).

2.4.5 Leucine Rich Repeat (in FLII) Interacting Protein 1

Leucine Rich Repeat (in FLII) Interacting Protein 1 (LRRFIP1) is normally found in cytosol and is able to detect B-form and Z-form dsDNA through its nucleic acid binding domain, resulting in production of Interferon-β (IFN-β) (Arakawa et al., 2010). It was suggested that LRRFIP1 may cooperate with β-catenin pathway to induce production of type 1 interferon as its expression was inhibited if β-catenin was knocked out.

On the other hand, LRRFIP1 has been reported as the repressor of TNF-α (a mediator for inflammation, apoptosis and development of secondary lymphoid organs) (Suriano et al., 2005). LRRFIP1 was able to associate with polymorphism site in TNF- α, resulting in exacerbation of autoimmune diseases. (Suriano et al., 2005). Besides that, LRRFIP1 was found mutated at high frequencies in breast cancer associated with disease progression (Sjöblom et al. 2006).

CHAPTER 3

MATERIALS AND METHOD

3.1 Cell Culture

Cell lines (NPC cell line and non-cancerous nasal epithelial cells) used in this study were obtained from the various laboratories that established the cell lines. Information on cells lines were summarized in Table 3.1.

All the cell lines were grown and maintained according to the recommended procedure by the author. In general, the cells were grown as adherent form in 75 cm^2 flask and maintained in 37ºC, 5% carbon dioxide (CO_2), 95% humidifying air incubator with appropriate recommended complete growth medium as shown in Table 3.2. The cells were cultured up to 70% to 90% confluence before subculture.

To subculture, the cells were washed with 1 X PBS (MP Biomedical, USA) and then 0.05% trypsin-EDTA (Gibco Invitrogen, USA) was added to culture flask. The cells were incubated at 37ºC, 5% carbon dioxide (CO_2), 95% humidifying air incubator for five minutes or until the cells detached from the flask with the aid of gentle tapping. Subsequently, 2 X volume of complete growth medium (with serum) was added (4 ml of complete medium was added

when 2 ml of trypsin-EDTA was used). The trypsinised cells were washed once in 10 ml complete growth medium before being used for subculture with 1:5 split ratios.

To cryopreserve, the cell pellet was resuspended in freezing medium (70% culture medium, 20 % fetal bovine serum and 10 % DMSO (Sigma, USA) at concentration about 1 x 10^6 viable cells/vial. The viable cells were then transferred into a sterile cryovial (Nunc, USA) and stored in CoolCell® Cell Freezing Containers (Biocision, USA) and subsequently placed overnight at -80 ºC before being placed into liquid nitrogen for long term storage.

Table 3.1: The cell lines used in the study and their background information.

NPC cells	Types	Name of NPC cell line	Description on the tissue origin	Presence of EBV	References
	Keratinizing squamous cell carcinoma	CNE1	Derived from a 58 year old women patient. The tumour had invaded the base of the skull with histological presentation of well differentiated squamous cell carcinoma.	Negative	(Chinese academic of laboratory science, 1978).
		TW01	The cells were stabilised from keratinizing squamous cell carcinoma NPC subtype.	Negative	(Lin et al., 1980)

Table 3.1 continued: The cell lines used in the study and their background information.

		HK1	Derived from a 17 year old Chinese male. Tumour was detected on the roof and left wall of the nasopharynx and had histological presentation of well differentiated squamous cell carcinoma.	Negative	(Huang et al., 1980)
	Non-keratinizing squamous cell carcinoma	CNE2	Patient was a 68 year old male patient and had histological presentation of poorly differentiated squamous cell carcinoma.	Negative	(Sizhong, Xiukung, & Yi, 1983)
		HONE 1	Established from biopsy specimen of poorly differentiated squamous cell carcinoma	Negative	(Yao et al., 1990)
	Undifferentiated carcinoma	TW04	Derived from undifferentiated carcinoma.	Negative	(Lin et al., 1980)
		TW06	Derived from undifferentiated carcinoma	Negative	(Lin et al., 1980)
		C6661	Derived from a subclone of C666 parental cells that were undifferentiated carcinoma.	Positive	(Cheung et al, 1999)

Table 3.1 continued: The cell lines used in the study and their background information.

Normal control	**Non-cancerous nasal epithelial cells**	NP69	Derived from biopsy from patient nasopharynx with symptoms of nasal obstruction and excessive bleeding	Negative	(Tsao et al. 2002)

Table 3.2: Cell lines and the recommended complete growth medium

NPC cell lines	**Complete growth medium**
TW01, TW04, TW06, C6661 and HONE 1	RPMI 1640 growth medium (Gibco Invitrogen, USA) supplemented with 10 % fetal bovine serum (Gibco Invitrogen, USA). and 50 U/ml penicillin (Gibco Invitrogen, USA),
CNE 1, CNE 2 and HK1	DMEM high glucose growth medium (Gibco Invitrogen, USA) supplemented with 10 % fetal bovine serum (Gibco Invitrogen, USA), and 50 U/ml penicillin (Gibco Invitrogen, USA).
NP69	Keratinocyte serum free medium (Gibco Invitrogen, USA) supplemented with 5 % fetal bovine serum (Gibco Invitrogen, USA), 50 U/ml penicillin (Gibco Invitrogen, USA), 25 µg bovine pituitary extract and 0.2 ng/ml recombinant egf

3.2 Pattern Recognition Receptors Gene Expression Study Using End Point Reverse Transcription-PCR (RT-PCR)

3.2.1 Cell Harvesting and RNA Extraction

The NPC cells and non-cancerous nasal epithelial cells NP69 were harvested at 80 % confluence and the total RNA was extracted using Trizol (Life technologies, US) Trizol was directly added to the culture flask and then allowed to stand at room temperature for five minutes. Cell pellet was shredded by five times passing through 21 G syringe needle. Next, cell suspension was centrifuged at 12000 rpm at 4 °C for 15 minutes. Carefully, the aqueous phase was transferred to a new 1.5 ml microcentrifuge tube. Then, 0.5 ml isopropanol was added into the aqueous phase and left at room temperature for 10 minutes before centrifugation at 12000 rpm for 15 minutes at 4 °C. At this point, a gel-like transparent pellet was visualised. The supernatant was discarded and the pellet was washed with 1 ml 70 % ethanol and followed by 1 ml 95 % ethanol. For each washing step, the pellet was centrifuged at 10000 rpm at 4°C for five minutes. The supernatant was discarded. After washing with 95 % ethanol, cell pellet was air dried at room temperature for 10-20 minutes. Air dried RNA pellet was dissolved in 20 µl of DEPC treated water containing Ribolock RNase Inhibitor (Thermo Scientific, USA). Before storage at -80 °C, the purity and quantity of the extracted total RNA were determined using NanoPhotometer (Implen, Germany) and the purity of total RNA was verified by agarose gel electropheresis. RNA with good purity was estimated by ratio of absorbance reading of 260:280 at range between 1.9 to 2.0. One µl

of each RNA was loaded onto 1 % agarose gel containing in 1 X TAE buffer. RNA was electrophoresed on the gel together with KAPA universal ladder (KAPA Biosystems, South Africa) at 60 Volts, 400 mAmp for one hour. Bands were visualised and image was captured using Advance Gel Imaging System (UVP, USA). The 18S and 28S RNA bands were expected to be seen in intact RNA sample.

3.2.2 Reverse Transcription for First Strand cDNA Synthesis

The cDNA was synthesised using 1 µg of total RNA extracted from each of the cell lines used in this study. Reverse transcription was carried out using RevertAid Reverse Transcriptase (Thermo Scientific, USA) according to recommended manufacturer protocol. The extracted RNA was added to reaction mixture consisting of 0.5 µg of Oligo $(dT)_{20}$ primers (Thermo Scientific, USA) and nuclease-free H_2O. The mixture was incubated at 65 °C for five minutes and chilled on ice for five minutes. Then, 200 units of RevertAid Reverse Transcriptase (Thermo Scientific, USA), 20 units of Ribolock RNase Inhibitor (Thermo Scientific, USA) and 2 µl of 10mM dNTPs were added to the mixture before incubation at 42 °C for one hour followed by 70 °C for 10 minutes. Generated cDNA was either used directly for detection of pattern recognition receptor genes or store at -80 °C for future use.

3.2.3 End Point Reverse Transcription- Polymerase Chain Reaction

End point reverse transcription - polymerase chain reaction (RT-PCR) was performed using DreamTaq DNA Polymerase (Thermo Scientific, USA) with a reaction volume of 20 µl containing the following components: 2 µl of 10 X DreamTaq Buffer with 20 mM $MgCl_2$, 0.4 µl of 10 mM dNTPs (Thermo Scientific, USA), 0.4 µl each of 10 µM forward and reverse primers (Information on primers and their sequences is covered in section 3.2.3.6 to 3.2.3.15), 0.5 U DreamTaq DNA Polymerase, 25 ng of cDNA and double distilled water (ddH_20). PCR was performed using the following PCR program on Veriti 96 well Thermal Cycler (Applied Biosystems, USA): initial denaturation at 95 °C for two minutes; followed by 30 cycles of denaturation at 95 °C for 30 seconds, annealing at 58 °C for 30 seconds, extension at 72 °C for 30 seconds; and final extension at 72 °C for two minutes.

After PCR, 10 µl of each reaction mixture was mixed with 1 X loading dye and loaded onto 2.0 % pre-stained agarose gel containing in 1 X TAE buffer. PCR mixture was electrophoresed on the gel together with GeneRuler 100 bp DNA Ladder (Thermo Scientific, USA) at 60 Volts, 400 mAmp for one hour. The gel was visualized and image was captured using Advance Gel Imaging System (UVP, USA). A single band is expected to be present indicating that RT-PCR process was working well.

3.2.3.1 Glyceraldehyde 3-phosphate dehydrogenase (GADPH)

GAPDH gene was used as a housekeeping gene for PCR. DreamTaq DNA Polymerase (Thermo Scientific, USA) was used to prepare the PCR reaction mixture. Highly purified salt-free primers for GAPDH (IDT, Singapore): forward primer, 5' AGGGCTGCTTTTAACTCTGGT 3'; reverse primer, 5' CCCCACTTGATTTTGGAGGGA 3' (Zhang et al., 2013) were used to amplify a 206 bp PCR product.

3.2.3.2 Beta-2 Microglubulin (B2M)

B2M gene was used as a housekeeping gene for quantitative real time-PCR. DreamTaq DNA Polymerase (Thermo Scientific, USA) was used to prepare the PCR reaction mixture. Highly purified salt-free primers for B2M (IDT, Singapore): forward primer, 5' GGCTATCCAGCGTACTCC A 3'; reverse primer, 5' ACGGCA GGCATACTCATC T 3' (Guo et al. 2010) were used to amplify a 247 bp PCR product.

3.2.3.3 18sRNA

Another housekeeping gene used in quantitative real time-PCR gene was 18sRNA. DreamTaq DNA Polymerase (Thermo Scientific, USA) was used to prepare the PCR reaction mixture. Highly purified salt-free primers for B2M (IDT, Singapore): forward primer, 5' TGTGCCGCTAGAGGTGAAATT

3’; reverse primer, 5’ TGGCAAATGCTTTCGCTTT 3’ (Kuchipudi et al. 2012) were used to amplify a 104 bp PCR product.

3.2.3.4 Toll Like Receptor 3 (TLR 3)

Primers were designed using primer 3 software. Highly purified salt-free primers for TLR3: forward primer, 5’ AGCCTTCAACGACTGATGC 3’ reverse primer, 5’ TTCCAGAGCCGTGCTAAG 3’ (synthesized by IDT, Singapore) were used to amplify a 200 bp PCR product.

3.2.3.5 Toll Like Receptor 4 (TLR 4)

Primers were designed using primer 3 software. Highly purified salt-free primers for TLR 4: forward primer, 5’ TGGACAATTTGGGCTAGAGG 3’ reverse primer, 5’ TTCCAGAGCCGTGCTAAG 3’ (synthesized by IDT, Singapore) were used to amplify a 196 bp PCR product.

3.2.3.6 Toll Like Receptor 6 (TLR 6)

Primers were designed using primer 3 software. Highly purified salt-free primers for TLR 6: forward primer, 5’ AGTAGCTGGGCTTGCATTGT 3’; reverse primer, 5’ TTATTGGAGGGCCTTGAGTG 3’ (synthesized by IDT, Singapore) were used to amplify a 200 bp PCR product.

3.2.3.7 Toll Like Receptor 9 (TLR 9)

Primers were designed using primer 3 software. Highly purified salt-free primers for TLR 9: forward primer, 5’ AAGGGGTGAAGGAGCTGTCT 3’; reverse primer, 5’ ACAGCAGCTACAGGGAAGGA 3’ (synthesized by IDT, Singapore) were used to amplify a 203 bp PCR product.

3.2.3.8 Toll Like Receptor 10 (TLR 10)

Primers were designed using primer 3 software. Highly purified salt-free primers for TLR 10: forward primer, 5’ GGCCAGAAACTGTGGTCAAT 3’; reverse primer, 5’ CTGCATCCAGGGAGATCAGT 3’ (synthesized by IDT, Singapore) were used to amplify a 199 bp PCR product.

3.2.3.9 Melanoma Differentiation-Associated protein 5 (MDA5)

Primers were designed using primer 3 software. Highly purified salt-free primers for MDA5: forward primer, 5’ GGAACATGCAGGCAGTTGAA 3’; reverse primer, 5’ CAAACGATGGAGAGGGCAAG 3’ (synthesized by IDT, Singapore) were used to amplify a 162 bp PCR product.

3.2.3.10 Retinoic acid-inducible gene I (RIG-I)

Primers were designed using primer 3 software. Highly purified salt-free primers for RIG-I: forward primer, 5’ AGAGCACTTGTGGACGCTTT 3’; reverse primer, 5’ TGCCTTCATCAGCAACTGAG 3’ (synthesized by IDT, Singapore) were used to amplify a 202 bp PCR product.

3.2.3.11 Absent in melanoma 2 (AIM 2)

Primers were designed using primer 3 software. Highly purified salt-free primers for AIM 2: forward primer, 5’ GCTGCACCAAAATCTCTCC 3’; reverse primer, 5’ ACATCCTGCTTGCCTTCT 3’ (synthesized by IDT, Singapore) were used to amplify a 163 bp PCR product.

3.2.3.12 Leucine Rich Repeat (In FLII) Interacting Protein 1 (LRRFIP 1)

Primers were designed using primer 3 software. Highly purified salt-free primers for LRRFIP 1 (IDT, Singapore): forward primer, 5’ CGGCAGCAGAAGGAGATCTA 3’; reverse primer, 5’ TTCCACGACTACCCACTGAC 3’ (synthesized by IDT, Singapore) were used to amplify a 169 bp PCR product.

3.2.3.13 DEAD-Box Helicase 41 (DDX41)

Primers were designed using primer 3 software. Highly purified salt-free primers for DDX41: forward primer, 5’ GCCCTTGTAAAGCCTGTGAC 3’; reverse primer, 5’ TTGAGCAGCAGGTACTCGTG 3’ (synthesized by IDT, Singapore) were used to amplify a 200 bp PCR product.

3.2.3.14 NLR family CARD domain-containing protein 4 (NLRC4)

Primers were designed using primer 3 software. Highly purified salt-free primers for NLRC4: forward primer, 5’ CTGCATCATTGAAGGGGAAT 3’; reverse primer, 5’ TGTCTGCTTCCTGATTGTGC 3’ (synthesized by IDT, Singapore) were used to amplify a 202 bp PCR product.

3.2.3.15 NOD-Like Receptor Family, Pyrin Domain Containing-3 Protein (NLRP3)

Primers were designed using primer 3 software. Highly purified salt-free primers for NLRP3: forward primer, 5’ CTTCTCTGATGAGGCCCAAG 3’; reverse primer, 5’ GCAGCAAACTGGAAAGGAAG 3’ (synthesized by IDT, Singapore) were used to amplify a 200 bp PCR product.

3.3 Quantitative Analysis of Pattern Recognition Receptor Using Quantitative Real Time Reverse Transcription –Polymerase Chain Reaction

3.3.1 Quantitative Real Time Reverse Transcription –Polymerase Chain Reaction

Quantitative real time- PCR (qRT-PCR) was performed using SYBR Select Master Mix (Life Technologies, USA). A reaction mixture with 20 µl in total volume was prepared with the following components: 10 µl of SYBR select master mix, 10 µM forward and reverse primers, 0.5 U DreamTaq DNA Polymerase, 20 ng of cDNA and ddH_20. qRT-PCR was performed using the following PCR program on iCycler (Bio-rad, US): initial denaturation at 95°C for two minutes; followed by 40 cycles of denaturation at 95 °C for 30 seconds, annealing at 60 °C for 30 seconds, extension at 72 °C for 30 seconds. Melting-curve analysis from temperature 60 °C to 95 °C was performed to ensure the specificity of the products

SYBR Green, a commonly used fluorescent DNA binding dye that binds to all double–stranded DNA, was used to detect and monitored the fluorescence signal throughout the cycle. SYBR Green has an excitation and emission maxima of 494 nm and 521 nm. No-template control and a no-RT control (RT negative) were included to verify that primer–dimer formation and genomic DNA contamination effects were negligible. Each sample was examined in duplicate and data presented were derived from two independent experiments.

3.3.2 Data Analysis of Quantitative Real Time PCR

Analyses of real-time RT-PCR products were performed using the iCycler software (Biorad, US). Relative quantification of mRNA amount was accomplished by comparative delta CT method (Schmittgen.et al, 2008). Non-cancerous nasal epithelial cells (NP69) were used as calibrators, i.e. as the basis for comparative results. Relative amounts of NPC cell lines mRNA were normalized to the average of two housekeeping genes namely Beta-2-Microglobulin (B2M) and 18 sRNA. The value was expressed relative to the calibrator using the arithmetic formula:

Fold change = $2^{-\Delta\Delta CT}$ (Livak & Schmittgen 2001)

$-\Delta\Delta CT = (CT_{\text{Target gene}} - CT_{\text{housekeeping gene}})_{\text{NPC cell line}} - (CT_{\text{Target gene}} - CT_{\text{housekeeping gene}})_{\text{NP69}}$

Note: CT = threshold cycle

In this study, results were presented as mean ± standard deviation of fold change relative to non-cancerous nasal epithelial cells (NP69). A bar chart of fold change versus NPC cell lines was used to illustrate the difference in expression of NPC cell lines relative to NP69. Asterisk was used to show the statistical significance in target gene expression.

3.4 Protein Expression Study Using Immunohistochemistry

3.4.1 Nasopharyngeal Carcinoma Cell and Normal Epithelial Cells (NP69) Harvesting and Fixation

The NPC cell lines and non-cancerous nasal epithelial cells (NP69) were cultured and expanded until 70 – 90% confluent in a 75 cm^3 cell culture flask. Then, the cells were harvested using 0.05 % trypsin-EDTA. Cells were resuspended in 1 X phosphate buffered saline (PBS) and centrifuged at 2000 rpm for 5 minutes. The supernatant was discarded and the cell pellet was fixed overnight in 10% formalin in PBS solution.

3.4.2 Cell Block Preparation

Formalin -fixed cells were transferred into a microcentrifuge tube and washed twice with 1 X PBS by centrifugation at 2000 rpm for 5 minutes to pellet the cells. One percent agarose was prepared by heating at high temperature using a microwave owen. The cooked agarose were let to cool a little and then 50 µl of the cooked agarose was transferred to the microcentrifuge tube. The cell pallets were resuspended by pipetting. The mixture was allowed to cool on ice and extracted by mild tapping. The cells were phased into a paraffin embedded tissue block in STP 120 Spin Tissue Processor Machine (Thermo Scientific, USA) according to standard tissue processing protocol.

3.4.3 Cell Block Processing Using the Tissue Processor Machine

Tissue processing was performed using STP 120 Spin Tissue Processor Machine (Thermo Scientific, USA). The extracted cell block was inserted into the processing cassette and placed in the tissue processor basket. The tissue processor machine was programmed according to the standard operating procedure which comprises a fixation step, dehydration step, cleaning step and wax infiltration step. The fixation step was performed by immersing the cell block cassette in formalin solution for two cycles, 1 hour each. This was followed by the dehydration step where the cell block samples were immersed in a series of graded ethanol, 70 % 80 % and 90 % for 1 hour and 30 minutes each and three cycles of 100 % ethanol for 1 hour each. Next, cell block cassettes were immersed in two cycles of xylene for 1 hour 30 minutes each. Lastly, wax infiltration was performed by immersing the cell block cassette for two cycles of melted paraffin for 2 hours each.

3.4.4 Paraffin-Embedding and Sectioning of Processed Cell Block

The processed cell block was pressed into a paraffin embedded tissue block using the Microm EC 350 Modular Tissue Embedding Center (Thermo scientific, USA). The melted paraffin was added into the mould through a pipeline onto the processed cell block. Then, the cassette was placed on the paraffinated cell block as cover. The cell block containing paraffin was placed on ice to harden. The hardened paraffin embedded cell block was then

sectioned using a HM 325 rotary microtome (Thermo scientific, USA) at thickness of 5 microns each and placed on the surface of water in a water bath at 40 ℃. Individual sections were fished using a glass microscope slide and allowed to dry. The glass slides with tissue sections were placed in a microscope slide storage box and stored at 4 ℃.

3.4.5 Standard Immunohistochemistry Staining Protocol

The samples slides were first heated using a hot plate at 60 ℃ for 20 minutes. The sample slides were then placed into staining rack and immersed in xylene twice for 10 minutes each. Once deparaffinised, the slides are rehydrated in graded ethanol (100 %, 80 % and 70 %). The slides were immersed in water twice for 5 minutes each before proceeding to the antigen retrieval step.

Heat-induced epitope retrieval was performed by heating the sample slides in tri sodium citrate buffer (10 mM sodium citrate, 0.05 % Tween 20, pH 6) at high temperature for 20 minutes using a microwave owen. Precaution was taken to replace the evaporated buffer to ensure the slides were not left dry. Upon completion, the slides were allowed to cool at room temperature. Then, the slides were washed three times in 1X Tris-buffered saline (50 mM Tris-Cl, pH 7.5, 150 mM NaCl) for 5 minutes each. Hydrophobic barrier pen (Sigma-Aldrich, USA) was used to encircle the area with tissue section in order to allow minimal use of reagents for subsequent staining steps.

Peroxidase blocking solution (Dako, Denmark) was added to the encircled area and allowed to stand for 15 minutes. The slides were washed three times in 1X Tris-buffered saline (TBS) for 5 minutes each. Subsequently, two drops of bovine serum albumin (0.2 %) were added to the encircled area and incubated for 1 hour to prevent non-specific binding of antibody. Next, the samples slides were incubated with primary antibody. After incubation, slides were washed three times in 1X TBS before proceeding to secondary antibody incubation.

Horseradish peroxide conjugated secondary antibody (Dako, Denmark) was added to the encircled area and incubated for 30 minutes and then washed three times with 1X TBS for 5 minutes each. Next for visualization, sample slides were incubated with DAB substrate solution (Dako, Denmark) for 5 minutes and washed three times with tap water for 5 minutes each. Positively stained sample slides were indicated by the brown staining while negatives would appear unstained. The samples slides were counter stained by immersing in hematoxylin for 3 minutes followed by washing using running tap water for 5 minutes. Hematoxylin was used to stain the nucleus of the cells.

Before mounting the sample slides, a dehydration step was performed by using immersing sample slide twice in graded ethanol (70 %, 95 % and 100 %) for 2 minutes each followed by two washes of xylene for 5 minutes each. Lastly, the stained slides were mounted using DPX mounting media (Merck, USA).

3.4.5.1 Toll Like Receptor 3 Primary Antibody

TLR 3 primary antibody (clone: 40C1285.6) (Thermo Fisher Scientific, USA) was added at concentration 1:800 to the encircled area and incubated overnight at 4 ℃. The slides were washed three times in 1X TBS prior to proceeding to next step.

3.4.5.2 Toll Like Receptor 4 Primary Antibody

TLR 4 primary antibody (clone: 76B357.1) (Thermo Fisher Scientific, USA) was added at concentration 1:1000 to the encircled area and incubated overnight at 4 ℃. The slides were washed three times in 1X TBS prior to proceeding to next step.

3.4.5.3 Toll Like Receptor 9 Primary Antibody

TLR 9 primary antibody (clone: 26C5593.2) (Thermo Fisher Scientific, USA) was added at concentration 1:1000 to the encircled area and incubated for one hour at room temperature. The slides were washed three times in 1X TBS prior to proceeding to next step.

3.4.5.4 Toll Like 6 Receptor Primary Antibody

TLR 6 primary antibody (clone: 86b1153.2) (Thermo Fisher Scientific, USA) was added at concentration 1:600 to the encircled area and incubated overnight at 4 ℃. The slides were washed three times in 1X TBS prior to proceeding to next step.

3.4.5.5 RIG-Like Receptor Protein Primary Antibody

RIG-I primary antibody (clone: 2M6F10) (Thermo Fisher Scientific, USA) was added at concentration 1:1000 to the encircled area and incubated overnight at 4 ℃. The slides were washed three times in 1X TBS prior to proceeding to next step.

3.4.5.6 DEAD Box Protein 41 Primary Antibody

DDX41 primary antibody (clone: EPR14298) (Thermo Fisher Scientific, USA) was added at concentration 1:100 to the encircled area and incubated overnight at 4 ℃. The slides were washed three times in 1X TBS prior to proceeding to next step.

3.4.5.7 NOD-Like Receptor Family, Pyrin Domain Containing-3 Protein Antibody

NLRP3 primary antibody (clone: 25N10E9) (Thermo Fisher Scientific, USA) was added at concentration 1:1000 to the encircled area and incubated overnight at 4 ℃. The slides were washed three times in 1X TBS prior to proceeding to next step.

3.5 Protein Expression Study using Western Blot

3.5.1 Sample Preparation

Cultured cells were harvested at 80 % confluence and detached from the culture flask using 0.05 % trypin EDTA. Harvested cells were resuspended in 1 X phosphate buffered saline (PBS) and centrifuged at 2000 rpm for 5 minutes. The supernatant was discarded and the cell pellets were lysed using lysis buffer along with protease and phosphatase inhibitors.

3.5.2 Bradford Assay

We first mixed 1 µl of sample protein with 100µl of Bradford assay reagent (Bio-Rad, USA) on a 96- well plate and each sample was prepared in duplicate. The samples were placed in microplate reader and measured at 595 nm. A standard curve using known protein standards was prepared by plotting

the 595 nm values (y-axis) versus their concentration in µg/ml (x-axis). The standard curve was then used to determine the concentration of unknown proteins.

3.5.3 SDS-PAGE Gel

We prepared a 5% or 10% separating gel based on the size of the protein of interest and added it to the gel cassette. When the separating gel had solidified, we prepared a stacking gel and poured it on top of the separating gel. The comb was placed on the stacking gel and then allowed to solidify. After the stacking gel had solidified, samples were prepared by mixing protein samples with SDS buffer at 6:1 ratio (sample: SDS buffer). Samples were heated at 95 °C for 10 minutes. Lastly, protein marker was loaded onto the first well followed by the rest of the samples on the SDS PAGE gel. The electrophoresis apparatus was used to run the gel at 200 V for 45 minutes.

3.5.4 Transferring Proteins from SDS PAGE Gel to PVDF Membrane

First the PVDF membrane was soaked in methanol for 5 minutes. Separately, the black sponge and white sponge were soaked in transfer buffer till they were completely wet. The transfer sandwich was stacked based on the recommended manufacturer's protocol. The transferring tank was filled with transfer buffer, then the transfer sandwich cassette and ice tray were inserted into the tank. The transfer was run at 200 milliampere for 23 minutes.

3.5.5 Antibody Incubation

The PVDF membrane containing the transferred proteins were blocked using TBST with 5 % BSA for 1 hour. After incubation, the PVDF membrane was rinsed three times in TBST. Each primary antibody was added separately at 1: 5000 ratio diluted in TBST with 1% BSA and then incubated overnight at 4 °C. After incubation, the PVDF membrane was rinsed three times with TBST. Then secondary antibody was added at 1: 8000 ratio diluted in TBST with 1% BSA and incubated for 2 hours. Lastly the PVDF membrane was rinsed 3 times in TBST before proceeding with imaging.

Table 3.3: Primary antibody information

Primary antibody	Clone	Specificity
TLR3	40C1285.6	Correspond to amino acids 55-70 (VLNLTHNQLRRLPAAN) of TLR3/CD283 protein.
TLR4	76B357.1	Correspond to amino acids 100-200 of human TLR4, isoform C, LPEYFSNLTNLEHL.
TLR9	26C5593.2	Correspond to residue surrounding Gly442 of human TLR9 protein.
RIG-I	2M6F10	Correspond to amino acid (31 PWFREEEVQYIQAEKNNKG 49) of RIG-I/DDx58 protein.
DDX41	EPR14298	Correspond to human DDX41 amino acid 600 to the C-terminus. The exact sequence is proprietary. Database link: Q9UJV9
NLRP3	25N10E9	Correspond to amino acid mnlpr3 NOD domain protein (AA-216-385)

3.5.6 Imaging and Data Analysis

Colorimetric detection method was used to detect protein of interest where substrate 3, 3'-diaminobenzidine (DAB) was added to the blot to react with HRP conjugated with secondary antibody. This reaction between HRP and DAB produced a brown coloured precipitate that was readily visible to the eye on the blot. Camera based imager was used to capture the image of the blot.

3.5.7 Statistical Analysis

Quantitative real time – PCR results were analysed using Statistical Package for Social Sciences (SPSS) version 17. Data was presented as mean ± standard error of mean for replicated experimental results. ANOVA was used to analyse statistically significant difference in PRR expression in NPC cell lines versus non-cancerous nasal epithelial cells and the statistical significance was set at $P < 0.05$.

CHAPTER 4

RESULTS

4.1 Detection of Pattern Recognition Receptors in NPC Cell Lines and Non-Cancerous Nasal Epithelial Cell (NP69) using End Point Reverse Transcription PCR

Through literature review, 15 pattern recognition receptors (PRRs) which were previously reported to be able to respond to viral origin antigens were identified to look at for their possible association with NPC development. The 15 PRRs namely TLR3, TLR4, TLR6, TLR7, TLR8, TLR9. TLR10, MDA5, RIG-I, DDX41, AIM2, LRRFIP1, ZBDP-1, NLRP3 and NLRC4 were subjected to end point reverse transcription (RT) – PCR for their expression in 8 NPC cell lines (TW01, TW04, TW06, CNE1. CNE2, HK1, HONE1 and C6661) and non-cancerous nasal epithelial cells (NP69). A summary of the result is shown in Table 4.1.

Table 4.1: Summary of PRR expression in NPC cell lines and non-cancerous nasal epithelial cell

PRR family	PRR family members	Gene transcript detected								
		NPC cells								Non-cancerous nasal epithelial cells (NP69)
		TW01	TW04	TW06	CNE1	CNE-2	HONE1	HK1	C6661	NP69
Toll like receptors (TLRs)	TLR3	√	√	x	√	√	√	√	√	√
	TLR4	x	√	x	√	√	√	x	√	x
	TLR6	x	√	√	√	√	√	√	√	√
	TLR7	x	x	x	x	x	x	x	x	x
	TLR8	x	x	x	x	x	x	x	x	x
	TLR9	x	√	x	x	x	x	x	√	x
	TLR10	x	√	x	√	x	x	√	√	x
RIG-I like receptors (RLRs)	MDA5	√	x	x	√	√	√	√	√	√
	RIG-I	√	x	x	√	√	√	√	√	√
cytosolic DNA sensor	DDX41	√	√	√	√	√	√	√	√	√
	AIM2	x	x	x	x	x	x	x	x	x
	LRRFIP1	x	√	√	x	√	√	√	√	√
	ZBDP 1	x	x	x	x	x	x	x	x	x
NOD-like receptors (NLRs)	NLRP3	x	√	x	x	x	x	x	x	√
	NLRC4	√	x	√	√	x	x	x	x	√

4.1.1 TLR3

Toll like receptor 3 (TLR3) primers shown in primer table (Appendix A) were used to amplify TLR3 genes in one clear band of approximately 200bp. Peripheral blood mononuclear cells (PBMC) express TLR3 and were used as positive control in this study. Clear to faint bands were observed in the majority of NPC cell lines and non-cancerous nasal epithelial cells (NP69) and intense bands were observed in HK1 and C6661.

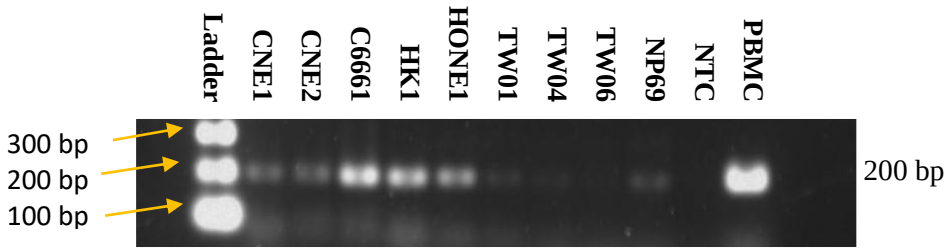

Figure 4.1: Amplification of TLR3 gene on eight NPC cell lines and NP69. Gel electrophoresis image of an end point RT-PCR showed intense band for TLR3 in C6661 and HK. 100 bp ladder was used to determine the size of the PCR product.

4.1.2 TLR4

Toll like receptor 4 (TLR4) primers shown in primer table (Appendix A) were used to amplify TLR4 genes in one clear band of approximately 196 bp in size. Peripheral blood mononuclear cells (PBMC) express TLR4 and were used as positive control in this study. Intense bands were observed in C6661 and NP69 but clear bands were presented in the majority of the NPC cell lines.

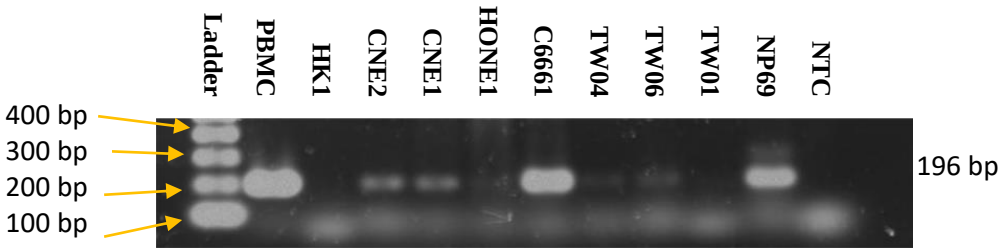

Figure 4.2: Amplification of TLR4 gene on eight NPC cell lines and NP69. Gel electrophoresis image of an end point RT-PCR showed intense band for TLR4 in C6661 and NP69. 100 bp ladder was used to determine the size of the PCR product.

4.1.3 TLR6

Toll like receptor 6 (TLR6) primers shown in primer table (Appendix A) were used to amplify TLR6 genes in one clear band of approximately 200 bp in size. Peripheral blood mononuclear cells (PBMC) express TLR6 and were used as positive control in this study. Except for TW01, clear bands were observed in all the NPC cell lines. Non-cancerous nasal epithelial cells (NP69) showed weak amplification of TLR6.

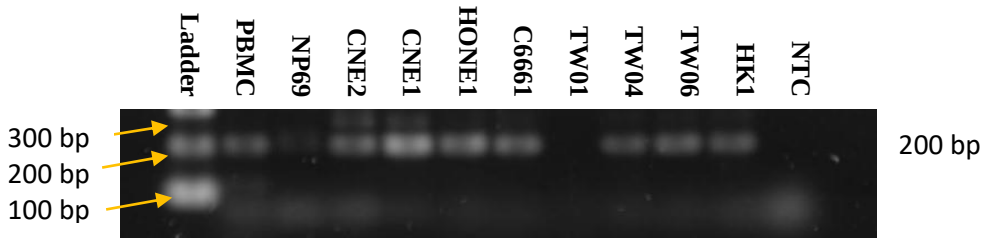

Figure 4.3: Amplification of TLR6 gene on eight NPC cell lines and NP69. Gel electrophoresis image of an end point RT-PCR showed bands for TLR6 in CNE1, CNE2, HONE1,C6661, TW01, TW04, TW06 and HK1. 100 bp ladder was used to determine the size of the PCR product.

4.1.4 TLR9

Toll like receptor 9 (TLR9) primers shown in primer table (Appendix A) were used to amplify TLR6 genes in one clear band of approximately 203 bp in size. Peripheral blood mononuclear cells (PBMC) express TLR9 and were used as positive control in this study. Clear bands were only observed in C6661 and TW04 NPC cell lines.

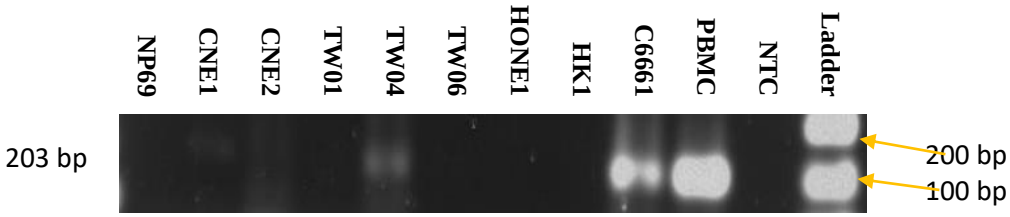

Figure 4.4: Amplification of TLR9 gene on eight NPC cell lines and NP69. Gel electrophoresis image of an end point RT-PCR showed intense band for TLR9 in C6661 and weak expression in TW04. 100 bp ladder was used to determine the size of the PCR product.

4.1.5 TLR10

Toll like receptor 10 (TLR10) primers shown in primer table (Appendix A) were used to amplify TLR6 genes in one clear band of approximately 199 bp in size. Peripheral blood mononuclear cells (PBMC) express TLR10 and were used as positive control in this study. Faint bands were observed in C6661, HK1, TW04 and CNE1 NPC cell lines. The rest of the NPC cells as well as the normal nasal epithelial cells showed no amplification of TLR10.

Figure 4.5: Amplification of TLR10 gene on eight NPC cell lines and NP69. Gel electrophoresis image of an end point RT-PCR showed intense band for TLR10 in PBMC but only a weak expression in C6661, HK1, TW01 and CNE1. 100 bp ladder was used to determine the size of the PCR product.

4.1.6 MDA5

Melanoma differentiation-associated gene 5 (MDA5) primers shown in primer table (Appendix A) were used to amplify MDA5 genes in one clear band of approximately 162 bp in size. Peripheral blood mononuclear cells (PBMC) express MDA5 and were used as positive control in this study. Intense bands could be observed in CNE1, TW01 and C6661 while faint bands were in the rest of the NPC cell lines. Non-cancerous nasal epithelial cells (NP69) also showed weak amplification of MDA5.

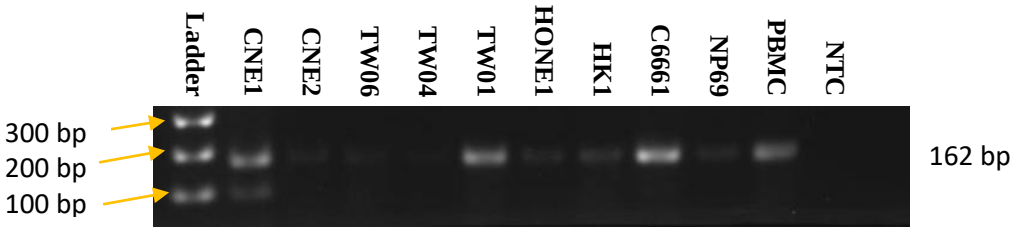

Figure 4.6: Amplification of MDA5 gene on eight NPC cell lines and NP69. Gel electrophoresis image of an end point RT-PCR showed intense band for MDA5 in C6661, CNE1, and TW01. 100 bp ladder was used to determine the size of the PCR product.

4.1.7 RIG-I

Retinoic Acid-Inducible Protein I (RIG-I) primers shown in primer table (Appendix A) were used to amplify RIG-I genes in one clear band of approximately 202 bp in size. Peripheral blood mononuclear cells (PBMC) express RIG-I and used as positive control in this study. Clear intense bands were shown in the majority of the NPC cell lines namely TW01, CNE1, CNE2, HK1 and C6661 and faint band in TW06 and TW04. Non-cancerous nasal epithelial cells showed presence of a faint band.

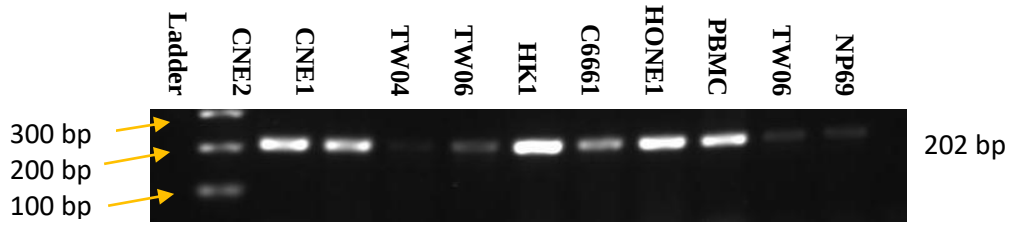

Figure 4.7: Amplification of RIG-I gene on eight NPC cell lines and NP69. Gel electrophoresis image of an end point RT-PCR showed intense band for RIG-I in all NPC cell lines with varying intensity. 100 bp ladder was used to determine the size of the PCR product.

4.1.8 DDX41

Dead Box Polypeptide 41 (DDX41) primers shown in primer table (Appendix A) were used to amplify DDX41 genes in one clear band of approximately 200 bp in size. Peripheral blood mononuclear cells (PBMC) express DDX41 and were used as positive control in this study. All the NPC cell lines as well as the non-cancerous nasal epithelial cells (NP69) expressed the DDX41.

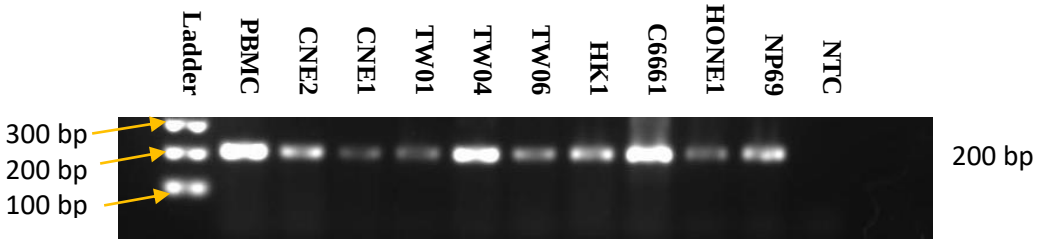

Figure 4.8: Amplification of DDX41 gene on eight NPC cell lines and NP69. Gel electrophoresis image of an end point RT-PCR showed intense band for DDX41 in all NPC cell lines and NP69 with varying intensity. 100 bp ladder was used to determine the size of the PCR product.

4.1.9 LRRFIP1

Leucine Rich Repeat (in FLII) Interacting Protein 1 (LRRFIP1) primers shown in primer table (Appendix A) were used to amplify LRRFIP1 genes in one clear band at approximately 169 bp. Peripheral blood mononuclear cells (PBMC) express LRRFIP1 and were used as positive control in this study. Except for CNE 1, most of the NPC cell lines had positive expression of LRRFIP1. Faint band was shown by non-cancerous nasal epithelial cells (Figure 4.9).

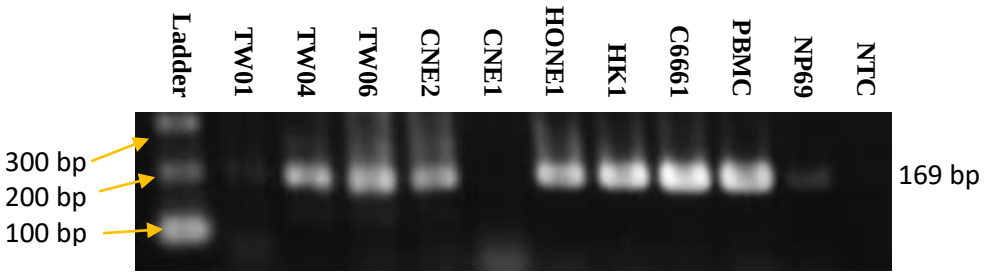

Figure 4.9: Amplification of LRRFIP1 gene on eight NPC cell lines and NP69. Gel electrophoresis image of an end point RT-PCR showed intense band for DDX41 in all NPC cell lines and NP69 with varying intensity. 100 bp ladder was used to determine the size of the PCR product.

4.1.10 NLRP3

NOD-Like Receptor Family, Pyrin Domain Containing-3 Protein (NLRP3) primers shown in primer table (Appendix A) were used to amplify NLRP3 genes in one clear band of approximately 200 bp in size. Peripheral blood mononuclear cells (PBMC) express NLRP3 and were used as positive control in this study. Intense band was shown in non-cancerous nasal epithelial cells (NP69). TW04 and TW06 had weak expression of NLRP3.

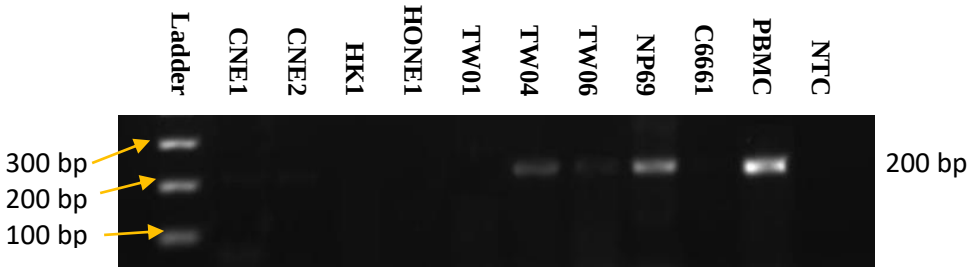

Figure 4.10: Amplification of NLRP3 gene on eight NPC cell lines and NP69. Gel electrophoresis image of an end point RT-PCR showed intense band for NLRP3 in NP69 and weak expression in TW04 and TW06. 100 bp ladder was used to determine the size of the PCR product.

4.1.11 NLRC4

NLRs family CARD domain-containing protein 4 (NLRC4) primers shown in primer table (Appendix A) were used to amplify NLRC4 genes in one clear band. Peripheral blood mononuclear cells (PBMC) express NLRC4 and were used as positive control in this study. Non-cancerous nasal epithelial cells (NP69) showed strong expression on NLRC4 whereas most of the NPC cells showed weak expression.

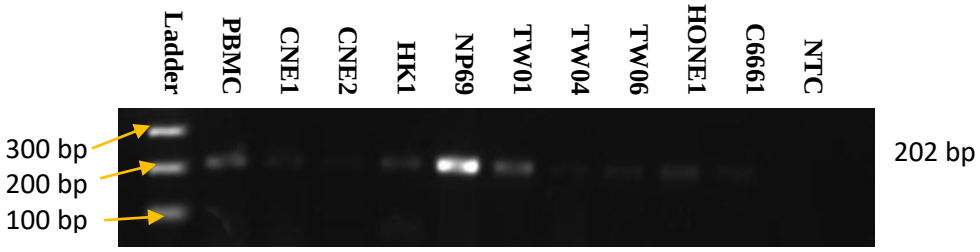

Figure 4.11: Amplification of NLRC4 gene on eight NPC cell lines and NP69. Gel electrophoresis image of an end point RT-PCR showed intense band for NLRC4 in NP69 and weak expression in all NPC cell lines. 100 bp ladder was used to determine the size of the PCR product.

4.2 Semi Quantitative Gene Expression Analysis of Selected Pattern Recognition Receptors in Nasopharyngeal Carcinoma Cells and Non-Cancerous Nasal Epithelial Cells (NP69) using Quantitative Real Time (qRT)-PCR

From the previous experiment, we identified 11 (out of 15) PRR that showed aberrant expression in NPC cell lines compared to non-cancerous nasal epithelial cells (NP69). From the identified 11 PRR, we selected 6 PRR namely, TLR3, TLR4, TLR9, RIG-I, DDX41 and NLRP3 to be further analysed using semi-quantitative real time (qRT) – PCR. All PRR gene expressions were normalized. We used the liwak method of data analysis against the average of two housekeeping genes, namely, 18s RNA and B2M. We calculated the fold change relative to non-cancerous nasal epithelial cells (NP69). The result was presented as mean fold change ± standard deviation and illustrated in the form bar chart of fold change relative to NP69 versus NPC cell lines in Figure 4.12 – 4.16. Asterisk was used to indicate the significant difference in expression of PRR in NPC cell lines compared to NP69. Positive fold change indicated upregulation in the expression of target gene while negative fold change indicated downregulation in the expression of target gene.

4.2.1 TLR3

End point RT-PCR revealed NPC cell lines and non-cancerous nasal epithelial cells can indeed express TLR3 (Figure 4.1). Out of all NPC cell lines tested C6661 had the highest fold change relative to non-cancerous nasal epithelial cells with 29.40 ± 1.26 and expression was significantly higher compared to nasal epithelial cells (NP69) ($p = 0.004$). HK1 also showed significant upregulation ($p = 0.00$) compared to NP69 with 8.61 ± fold. The cell line C6661 was the only cell line reported to harbour EBV (Cheung et al. 1999) while HK1 cell line was originated from a patient with recurrent non-keratinizing squamous cell carcinoma. Other NPC cell lines namely CNE1, CNE2, TW01, TW04, TW06 and HONE had downregulated expression compared to NP69 (Figure 4.12).

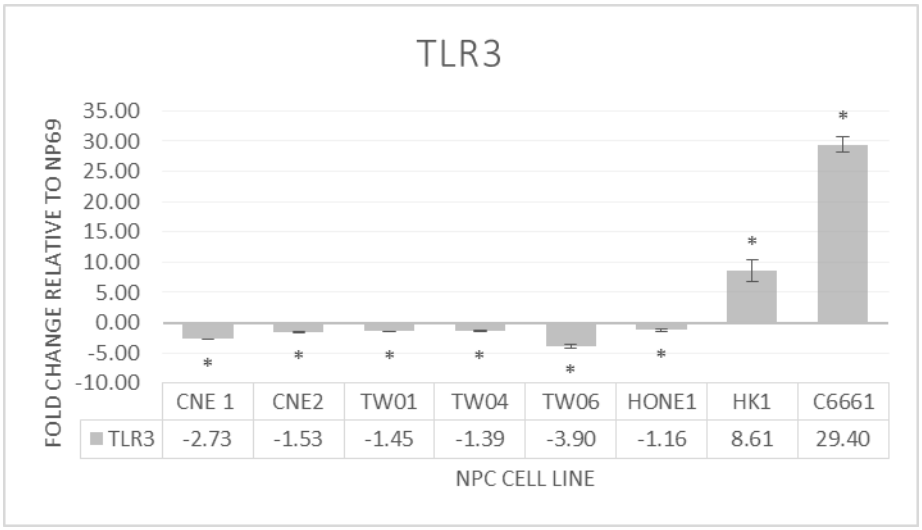

Figure 4.12: Semi quantitative toll like receptor 3 (TLR3) expression in NPC cell lines and non-cancerous NP69. TLR3 expressions were normalized against the average of housekeeping genes 18sRNA and B2M. The fold change relative to NP69 was determined using the formula delta-delta CT (-2^{DDCT}). TLR3 expression was upregulated in HK1 and C6661.

4.2.2 TLR 4

TLR4 was expressed at varying levels in NPC cell lines as previously shown in Figure 4.2. When analysed semi-quantitatively using qRT –PCR, we again noticed C6661 had the highest fold change relative to NP69 which was 167.78 ± 28.2 fold (p = 0.00). There was a slight positive fold change relative to NP69 in CNE1 (1.20 ± 0.05 fold) HONE1 (1.24 ± 0.21 fold) and HK1 (1.4 ± 0.93 fold). The other NPC cell line showed negative fold change relative to NP69 (Figure 4.13).

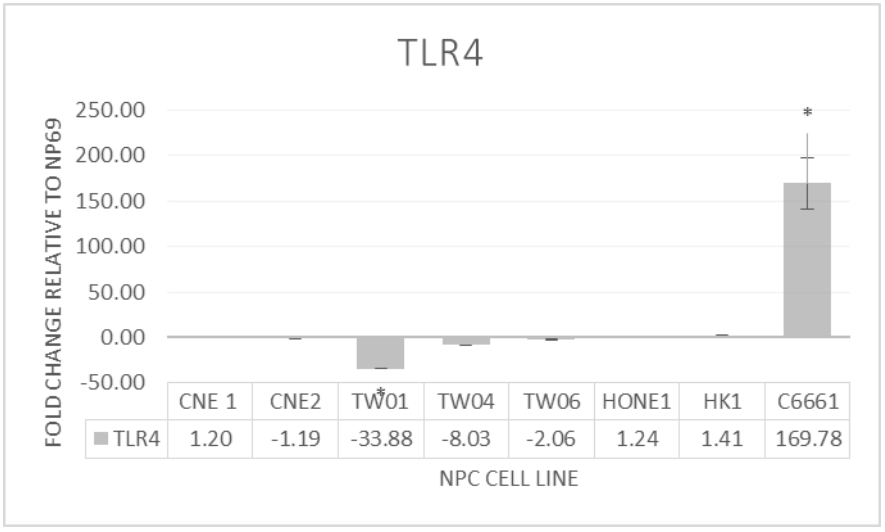

Figure 4.13: Semi quantitative toll like receptor 4 (TLR4) expression in NPC cell lines and non-cancerous nasal epithelial cell (NP69). TLR4 expressions were normalized against the average of housekeeping genes 18sRNA and B2M. The fold change relative to NP69 was determined using the formula delta-delta CT (-2^{DDCT}). Significantly high expression was shown in C6661.

4.2.3 TLR9

TLR9 expression was upregulated in C6661 cell line with 4.34 ± 0.23 fold but showed significant downregulation in the other NPC cell lines (Figure 4.14).

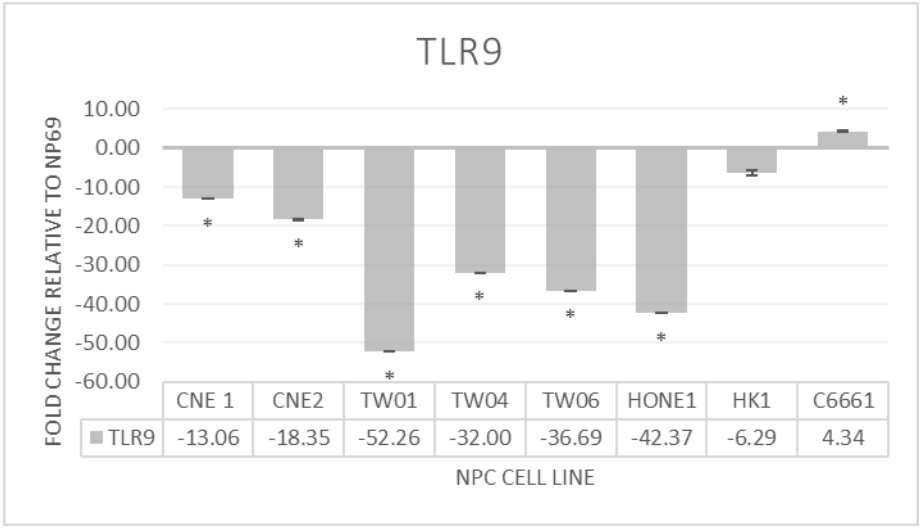

Figure 4.14: Semi quantitative toll like receptor 9 (TLR9) expression in NPC cell lines and NP69. TLR9 expressions were normalized against the average of housekeeping genes 18sRNA and B2M. The fold change relative to NP69 was determined using the formula delta-delta CT (-2^{DDCT}). TLR9 was upregulated in C6661 but downregulated in other NPC cell lines.

4.2.4 RIG-I

Relative to NP69, RIG-I expression was reported to be upregulated in all tested NPC cell lines at various degrees. Significantly high RIG-I expression was shown in CNE2 (p =-0.00) with 7.66 ± 2.45 fold and HK1 (p =0.00) with 7.52 ± 1.77 fold. Other NPC cells showed upregulation relative to NP69 (Figure 4.15).

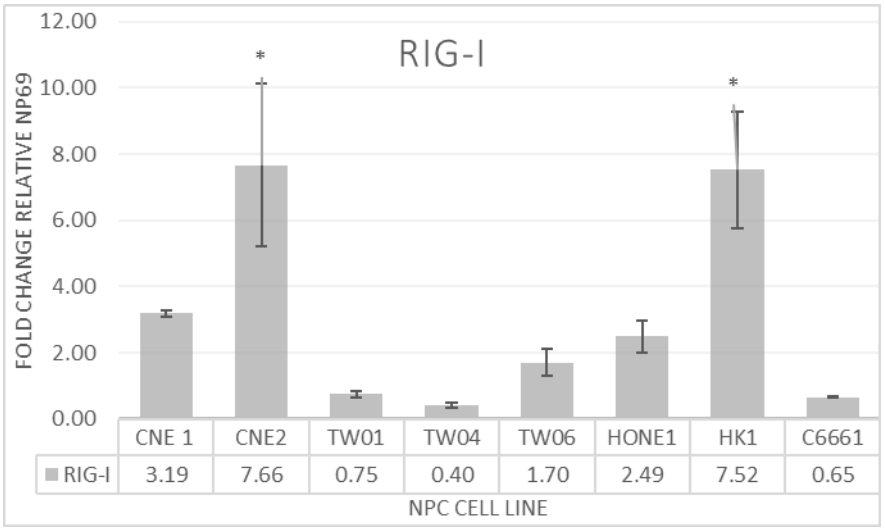

Figure 4.15: Semi quantitative retinoic acid-inducible Gene (RIG) - I like receptor (RIG-I) expression in NPC cell lines and NP69. RIG-I expressions were normalized against the average of housekeeping genes 18sRNA and B2M. The fold change relative to NP69 was determined using the formula delta-delta CT (-2^{DDCT}). Positive fold change indicates upregulation while negative fold change value indicated downregulation. RIG-I was upregulated in NPC cell lines relative to NP69.

4.2.5 DDX41

DDX41 had shown an intense expression in NPC cell lines when tested with RT-PCR (Figure 4.8). We found DDX41 expression was upregulated in the NPC cell lines in relative to NP69. All except for CNE1 (3.00 ± 0.63 fold) had significantly (p = 0.00) high expression compared to NP69 (Figure 4.16).

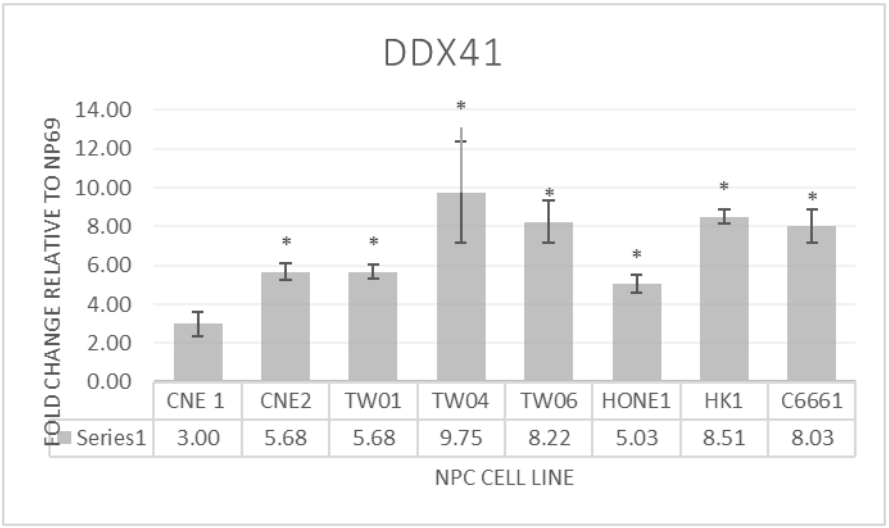

Figure 4.16: Semi quantitative dead box polypeptide 41 (DDX41) expression in NPC cell lines and NP69. DDX41 expressions were normalized against the average of housekeeping genes 18sRNA and B2M. The fold change relative to NP69 was determined using the formula delta-delta CT (-2^{DDCT}). DDX41 was upregulated in all NPC cells relative to NP69

4.2.6 NLRP3

As shown in Figure 4.10. NLRP3 showed a more intense single band in non-cancerous nasal epithelial cells but faint bands were observed in some NPC cells such as TW04 and TW06 and absent in the rest of the tested NPC cell lines. Using qRT –PCR, we further analysed the NLRP3 gene expression to determine whether its expression was truly absent in NPC cell lines. Relative to NP69, we observed significant ($p = 0.00$) downregulation of CNE2 (-13.26 ± 0.11 fold), TW01 (-32.7 ± 4.04 fold), TW04 (-12.59 ± 2.88), TW06 (-15.95 ± 1.22 fold), HONE1 (-6.29 ± 2.19 fold) and C6661 (-10.54 ± 1.55 fold). In summary NLRP3 was downregulated in all tested NPC cell lines compared to NP69 (Figure 4.17).

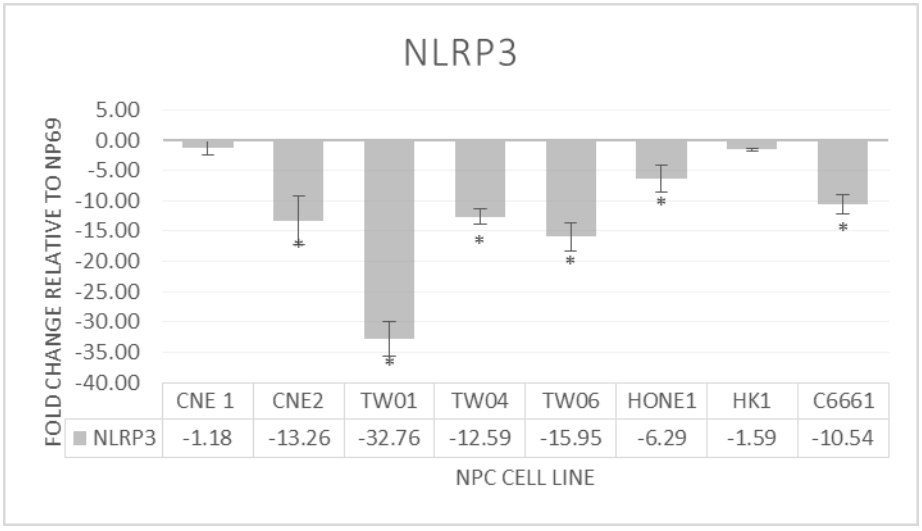

Figure 4.17: Semi quantitative NOD-Like receptor family, pyrin domain containing-3 protein 3 (NLRP3) expression in NPC cell lines and NP69. NLRP3 expressions were normalized against the average of housekeeping genes GADPH and B2M. The fold change relative to NP69 was determined using the formula delta-delta CT (-2^{DDCT}). NLRP3 was found downregulated in NPC cell lines compared to NP69.

4.3 Protein Expression Analysis of Selected Pattern Recognition Receptor

Next, we performed protein expression analysis to confirm whether the expressed genes were being translated into functional proteins. Western blot and Immunohistochemistry were performed. Despite both being the protein expression analysis methods, the immunohistochemistry protocol was established as we could use it for future study using paraffin embedded NPC patient tissue samples. Western blot being the gold standard for protein analysis, could be used to further validate the reliability of immunohistochemistry method.

4.3.1 TLR3

Result from qRT –PCR (Figure 4.12) showed TLR3 gene expression significantly upregulated in C6661 but slightly upregulated in and HK1. When analysed with western blot, similar result was obtained with intense band seen in C6661 lane and faint bands in CNE1 and HK1 as shown in Figure 4.18. With IHC, we saw a more intense brown staining in C6661 followed by HK1. Mild brown staining can still be observed in TW01, TW04, TW06 and HONE1.

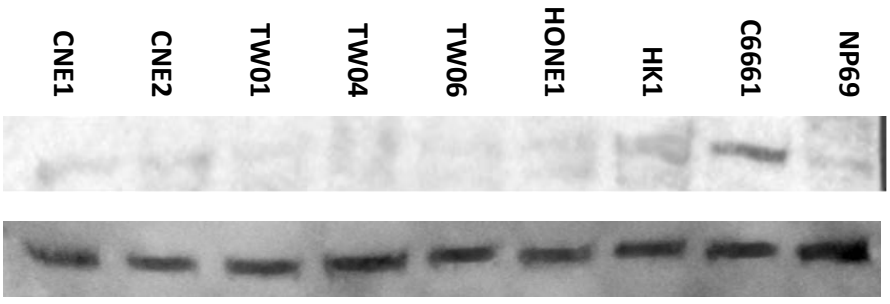

Figure 4.18: TLR3 protein expression in NPC cell line and NP69 using western blot. B-actin was used as positive control. Intense band indicated by C6661 while bands could be shown in CNE1 and HK1.

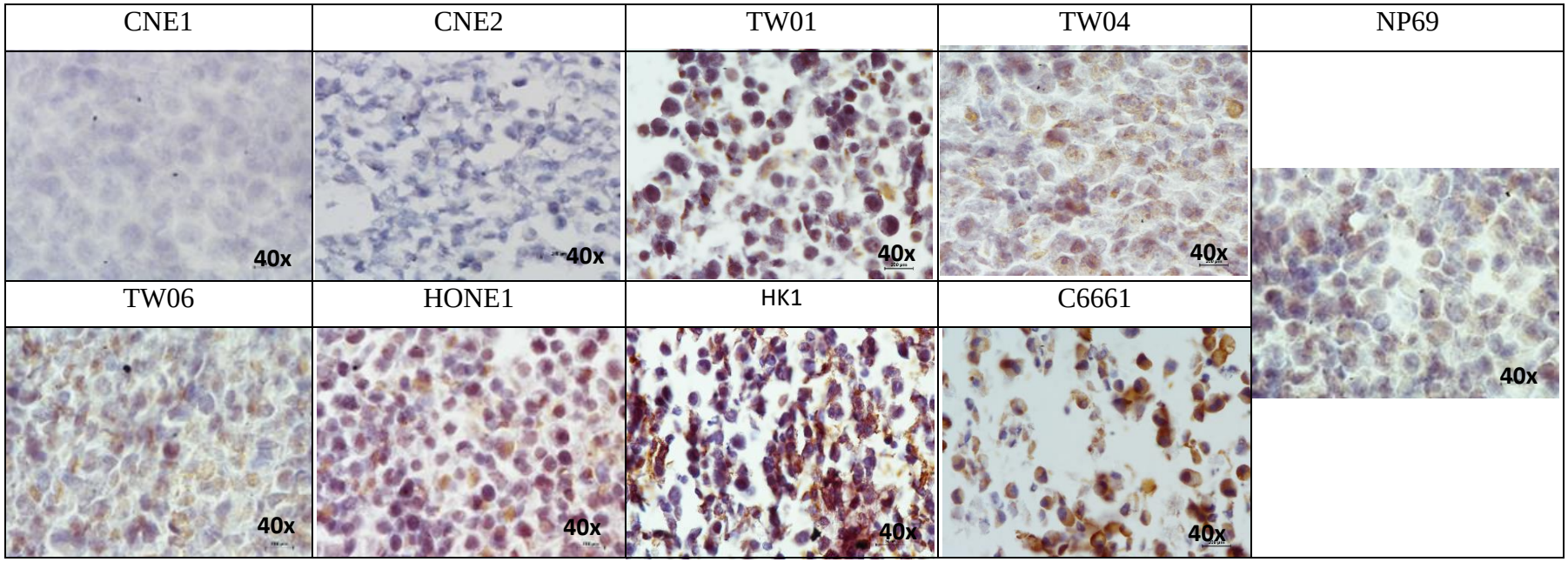

Figure 4.19: Immunohistochemistry (IHC) staining of TLR3 in NPC cells and non-cancerous nasal epithelial cells (NP69). The brown staining indicated positive staining for TLR3 and the nucleus was stained blue by hematoxylin. Intense brown staining was shown in C6661 followed by HK1 cell line. Milder staining was observed in TW01, TW04, TW06, HONE1 and NP69 compared to C6661. CNE1 and CNE2 did not show any staining. Image at 40x magnification and scale bar at 25μm.

4.3.2 TLR4

In Figure 4.13, TLR4 showed high expression in C6661 but minimally upregulated expression in CNE1, HONE1 and HK1. The protein analysis showed similar expression pattern with intense band for TLR4 in C6661 using western blot (Figure 4.20) which is further confirmed by result in IHC with the presence of intense brown staining in C6661 (Figure 4.21).

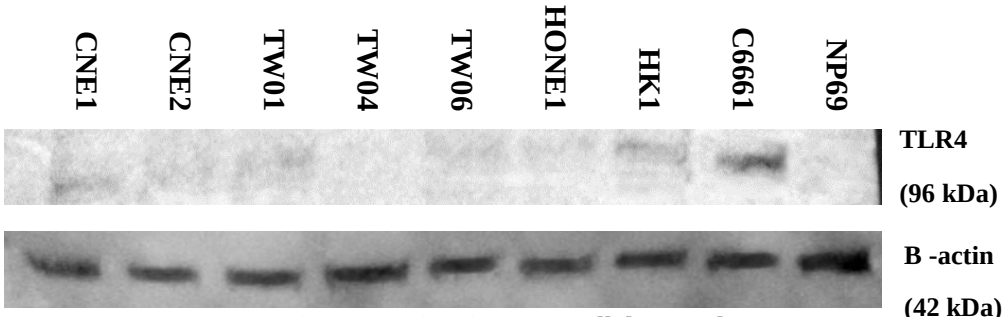

Figure 4.20: TLR4 protein expression in NPC cell line and NP69 using western blot. B-actin was used as positive control. There is an intense band in C6661 lane and a mild band in HK1 lane.

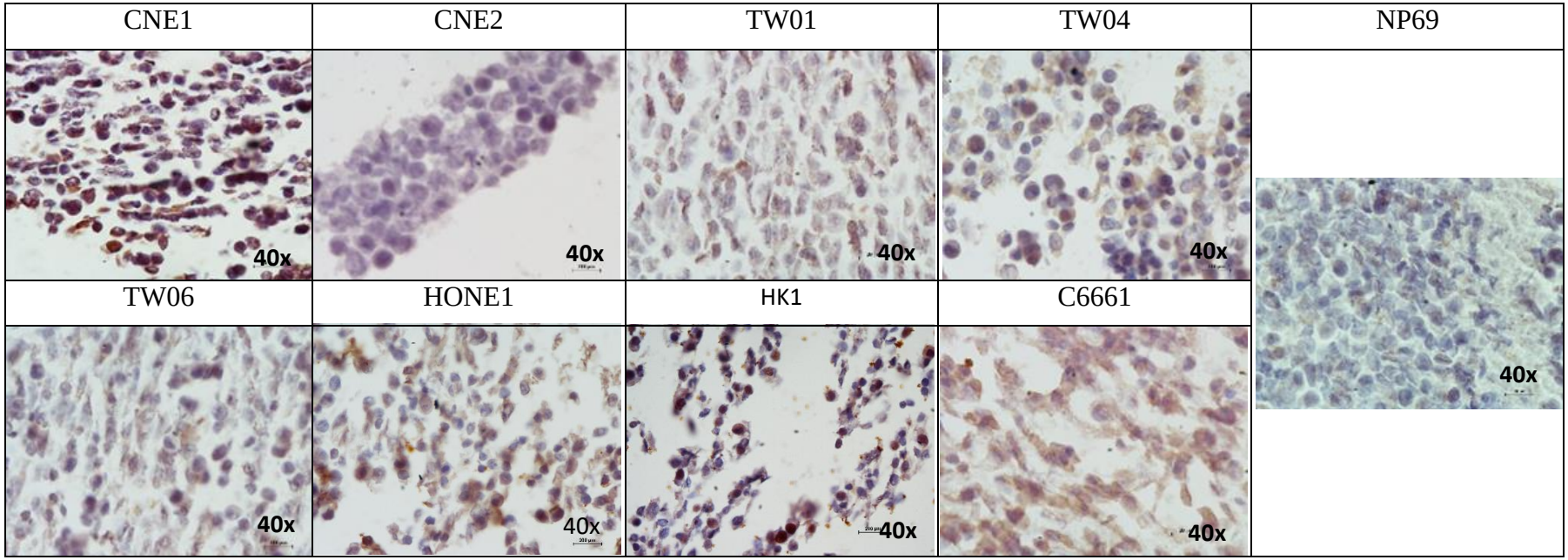

Figure 4.21: Immunohistochemistry (IHC) staining of TLR4 in NPC cells and non-cancerous nasal epithelial cells (NP69). The brown staining indicated positive staining for TLR4 and the nucleus was stained blue by hematoxylin. Intense brown staining could be seen in C6661 compared to other NPC cells. Very mild staining was observed in NP69. Image at 40x magnification and scale bar at 25μm.

4.3.3 TLR9

TLR9 gene expression was shown downregulated in NPC cell without EBV but upregulated in C6661, NPC cell with EBV. We did indeed find TLR9 protein expressed in C6661 cells shown using western blot (Figure 4.22) and IHC (Figure 4.23). Other than that, a mild band was observed in HK1 lane (Figure 4.22) but no TLR9 protein expression was detected in other NPC cell lines.

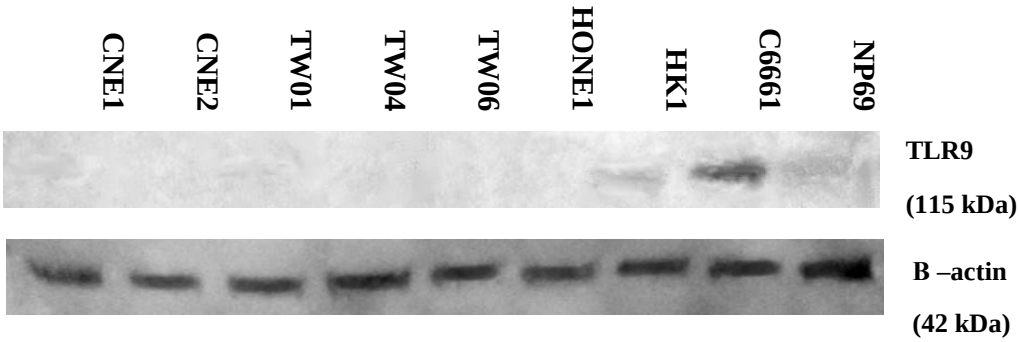

Figure 4.22: TLR9 protein expression in NPC cell lines and NP69 using western blot. B-actin was used as positive control. C6661 lane showed the presence of an intense band.

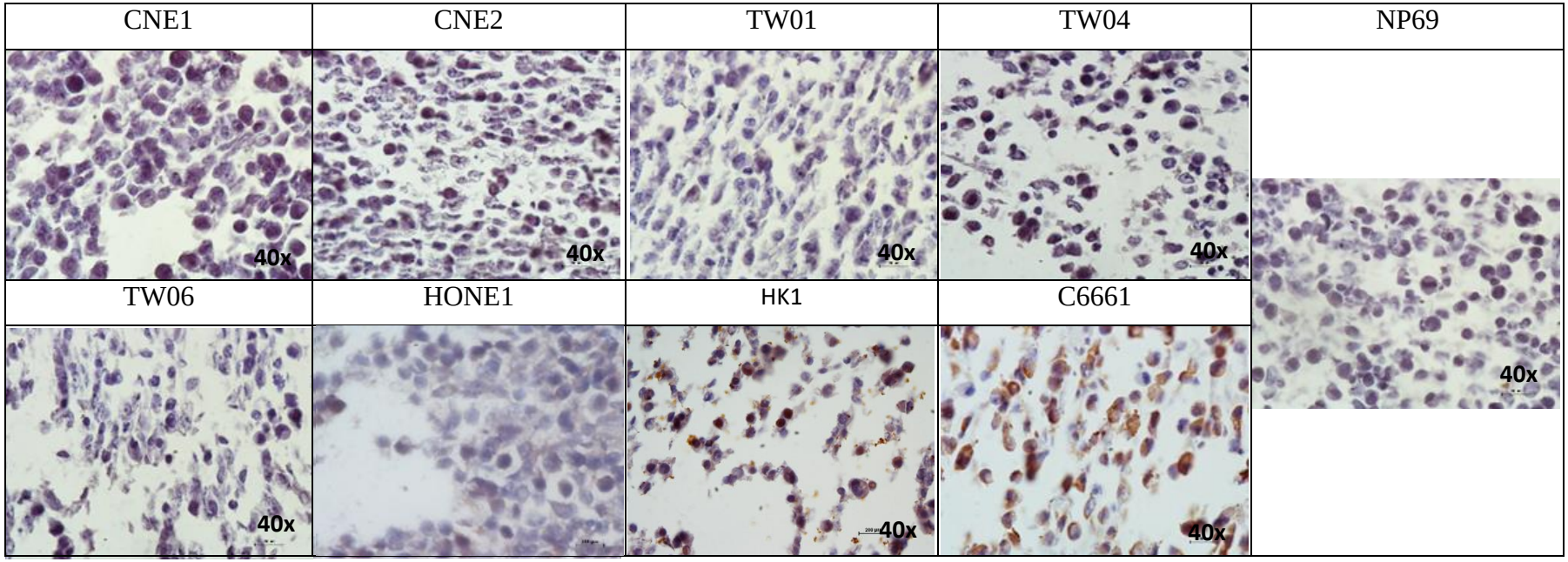

Figure 4.23: Immunohistochemistry (IHC) staining of TLR9 in NPC cells and non-cancerous nasal epithelial cells (NP69). The brown staining indicated positive staining for TLR9 and the nucleus was stained blue by hematoxylin. Intense brown staining showed in C6661 cells and a milder brown staining in HK1. The rest of the NPC cells and NP69 cell line had no staining. Image at 40x magnification and scale bar at 25µm.

4.3.4 RIG-I

RIG-I had shown a pattern of upregulation in gene expression in NPC cell lines compared to non-cancerous nasal epithelial cells. CNE2 and HK1 particularly had high expression of RIG-I and comparison of this result to its protein expression analysis using western blot showed clear bands in four of the NPC cells namely CNE1, CNE2, HK1 and HONE1 (Figure 4.24). This result was further supported by our result with IHC where brown staining was more apparent with CNE1, CNE2, and HK1, HONE1 compared to TW01, TW04, TW06 and C6661 (Figure 4.25).

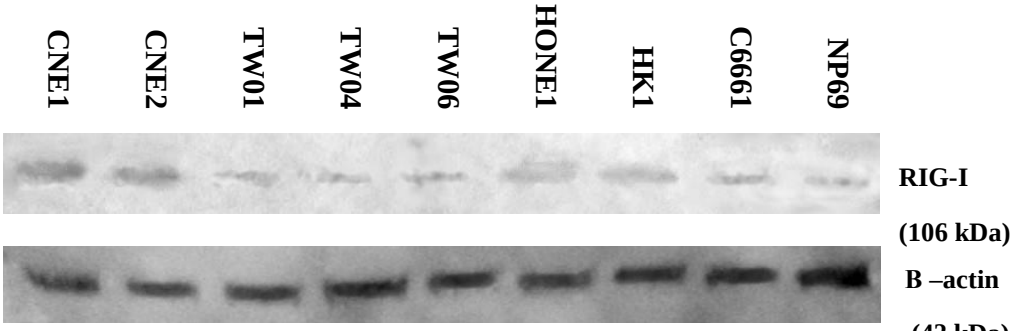

Figure 4.24: RIG-I protein expression in NPC cell line and np69 using western blot. B-actin was used as positive control. Bands at varying intensities were found in NPC cells and NP69.

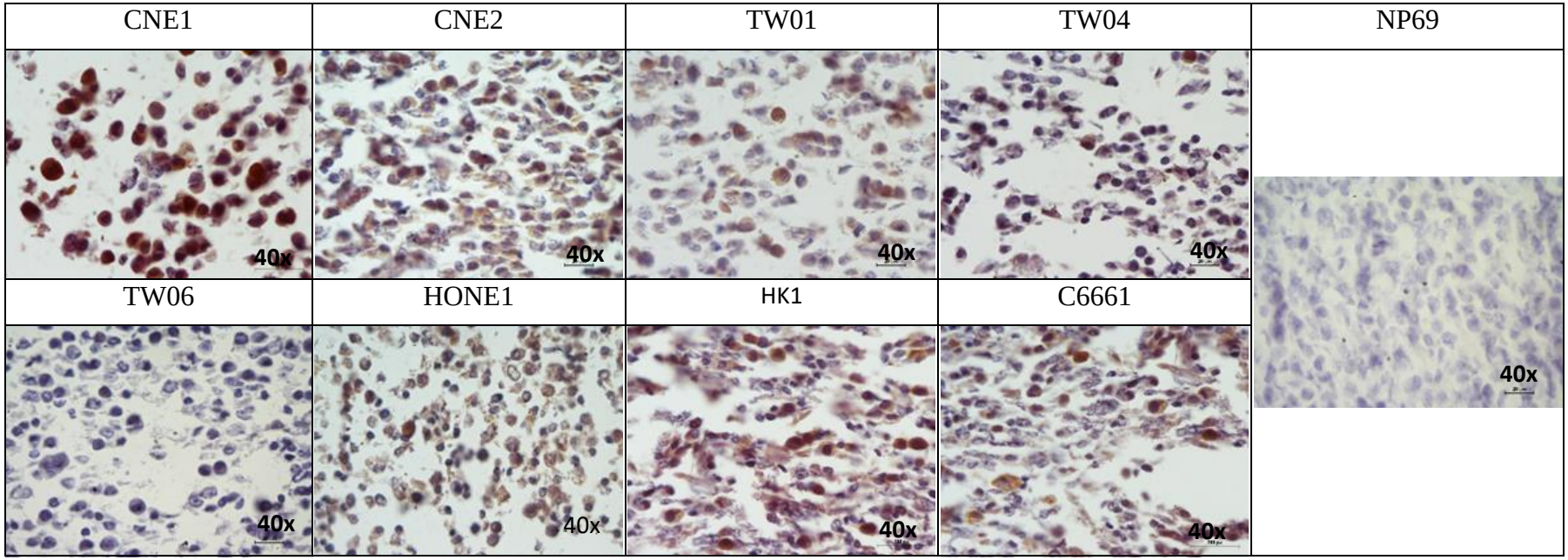

Figure 4.25: Immunohistochemistry (IHC) staining of RIG-I in NPC cells and non-cancerous nasal epithelial cells (NP69). The brown staining indicated positive staining for RIG-I and the nucleus was stained blue by hematoxylin. Brown staining could be seen in CNE1, CNE2, TW01, TW04, HONE1, HK1 and C6661. No staining was observed in TW06 and NP69. Image at 40x magnification and scale bar at 25μm

4.3.5 DDX41

Correlating gene expression analysis of DDX41 with protein expression analysis using western blot showed a similar pattern where all the tested NPC cell lines had upregulation in expression as shown in Figure 4.26. When we compared the western blot result with the IHC result, DDX41 protein expression was present in all NPC cell lines at varying intensities (Figure 4.27).

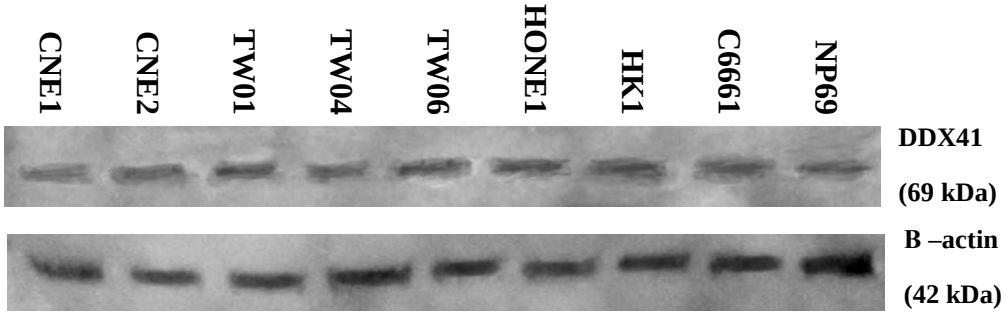

Figure 4.26: DDX41 protein expression in NPC cell line and NP69 using western blot. B-actin was used as positive control. Clear bands was shown in NPC cells and NP69**.**

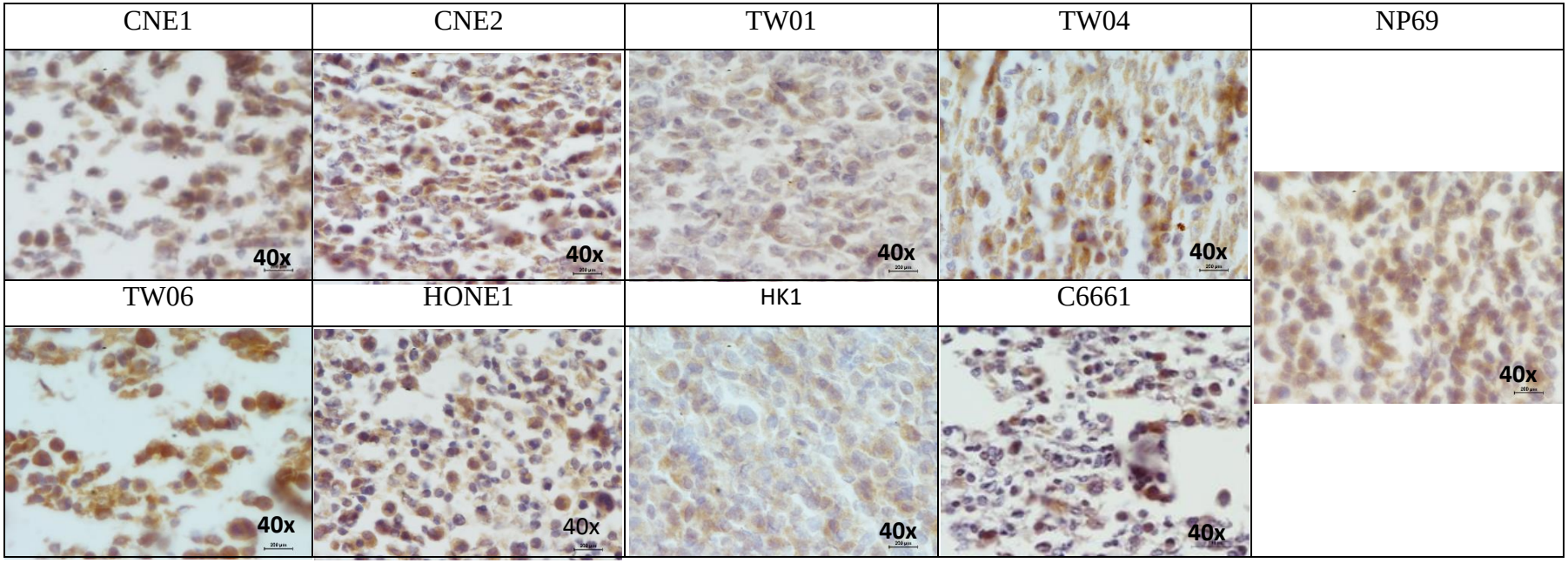

Figure 4.27: Immunohistochemistry (IHC) staining of DDX41 in NPC cells and NP69. The brown staining indicated positive staining for DDX41 and the nucleus was stained blue by hematoxylin. All the NPC cells and NP69 cell lines had brown staining. Staining was milder in HK1, C6661 and TW01. Image at 40x magnification and scale at bar at 25μm

4.3.6 NLRP3

NLRP3 gene did not show expression in NPC cell lines and RT-PCR result showed a band in non-cancerous nasal epithelial cells (Figure 4.10). A single band was observed in western blot for non-cancerous nasal epithelial cells (NP69) but no bands were present for all the NPC cell lines as shown in figure 4.28. IHC result further supports that NLRP3 protein was indeed expressed in NP69 which is shown as brown staining in figure 4.29. No brown staining was shown with IHC on all the tested NPC cell lines making it apparent that NLRP3 protein was not expressed.

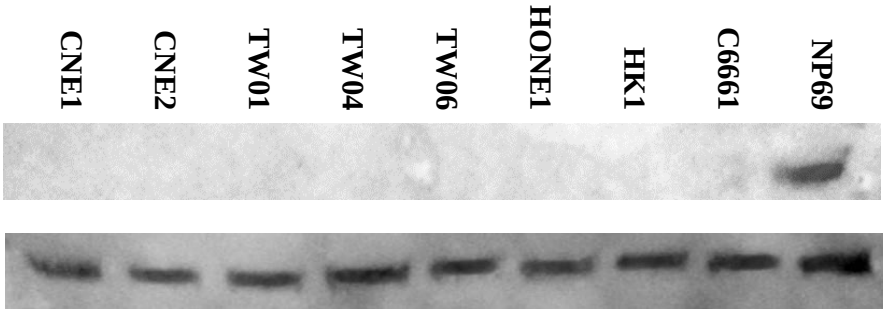

Figure 4.28: NLRP3 protein expression in NPC cell line and NP69 using western blot. B-actin was used as positive control. Intense band was shown in NP69 but no band was present for NPC cells.

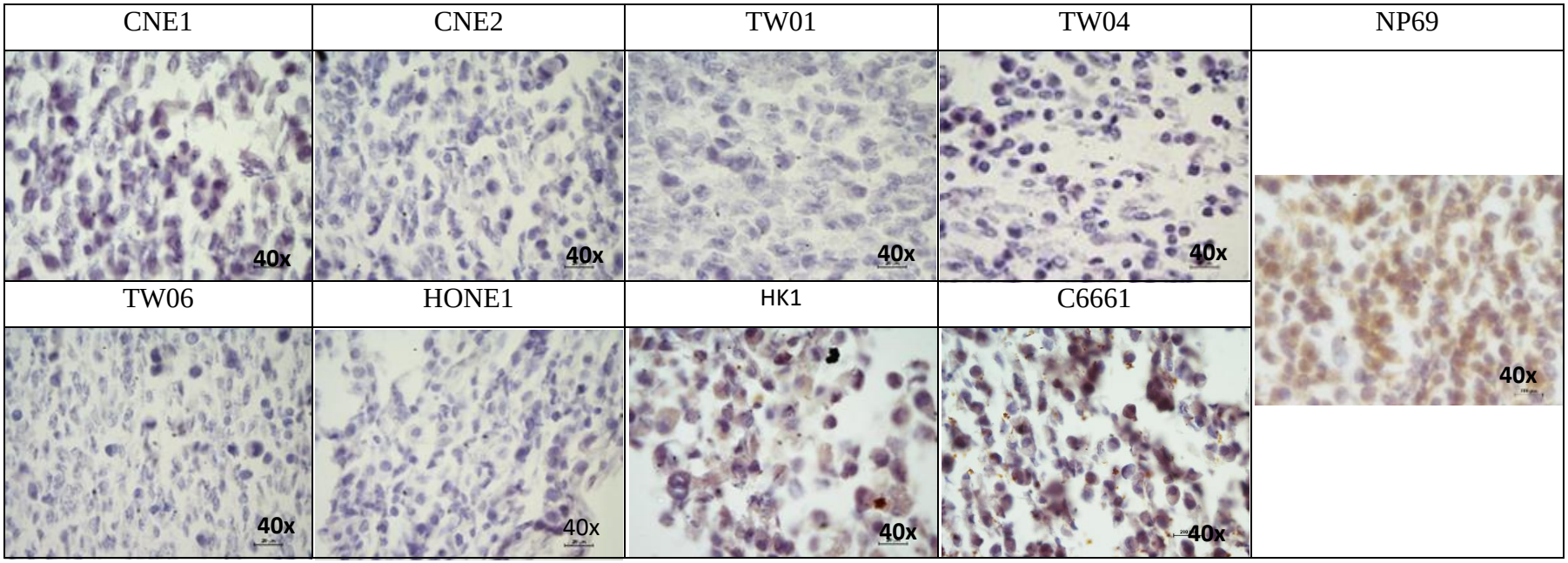

Figure 4.29: Immunohistochemistry (IHC) staining of NLRP3 in NPC cells and non-cancerous nasal epithelial cells (NP69). The brown staining indicated positive staining for NLRP3 and the nucleus was stained blue by hematoxylin. Brown staining could be observed in NP69 but is absent in all the NPC cell lines. Image at 40x magnification and scale bar at 25μm

CHAPTER 5

DISCUSSION

A panel of NPC cell lines (CNE1, CNE2, TW01, TW04, TW06, HONE1 HK1 and C66661) that are made up of tumour cells at different tumour grades and a non-cancerous nasal epithelial cells (NP69) were selected and used for the study. Detailed information about the properties of these cell lines are highlighted in Table 3.1.

Using RT-PCR, we were able to identify and narrow down PRRs that were expressed in NPC cell lines and non-cancerous nasal epithelial cells. For the TLRs family, aberrant expression was noted in 5 (out of 7) members namely TLR3, TLR4, TLR6, TLR9 and TLR10. It was apparent that C6661 cell line expressed higher levels of TLR3, TLR4 and TLR9 compared to other NPC cells. The properties that make C66661 cell line different from other NPC cells was the presence of EBV shown with long term culture as shown in Table 3.1. This result suggested TLR3, TLR4 and TLR9 were upregulated specifically in NPC cells with EBV, thus indicate possible association between these TLRs and EBV infection in NPC. We also noted that our results for CNE1 and CNE2 were consistent with a previously reported study, where faint bands for TLR4 were shown in CNE1 and CNE2 cell lines (Figure 4.2) while absent for TLR9 (Figure 4.4) (Zhang et al., 2009). The rest of the NPC cells

only showed low levels of TLRs expression. On the other hand, TLR6 was found at detectable levels in NPC cell lines (CNE1, CNE2, TW04, TW06, HK1, HONE1, and C6661). These appeared to be more intense compared to NP69 indicating possible aberrant expression. TLRs namely TLR7 and TLR8 were also tested for their expression using RT-PCR but were found not expressed in NPC cells lines nor the non-cancerous nasal epithelial cell (NP69).

RLR family members showed more promising results as targets of further investigation, particularly RIG-I which was identified to be expressed in all the NPC cell lines we tested (Figure 4.7). RIG-I was reported to be expressed lower in epithelial cells or resting cells which supports our finding for their low expression in non-cancerous nasal epithelial cells (NP69) (Loo & Gale 2011). Aberrant expression of DDX41 and LRRFIP1 was observed in NPC cell lines and non-cancerous nasal epithelial cells (NP69). The function of both PRR as cytosolic DNA sensor protein was only recently discovered (Zhiqiang et al., 2012; Yang et al., 2010). Aberrant expression LRRFIP1 was shown to promote metastasis in mouse xenograft model with colorectal cancer cells (Ariake et al. 2016). Both DDX41 and LRRFIP1 were promising candidates for further investigation of their gene and protein expression in NPC cells.

On the other hand, members of NLRs namely, NLRP3 and NLRC4 were both found at lower level in NPC cell lines compared to non-cancerous nasal epithelial cells (NP69). NP69 had clear bands for NLRC4 and NLRP3 (Figure 4.10 and 4.11). Lastly, we had also investigated expression of PRRs namely AIM2 and ZBDP-1 and found no expression of these genes in all of the tested NPC cell lines and NP69. Perhaps, AIM2 and ZBDP-1 may not play a significant role in NPC pathogenesis.

5.1 TLR3

In our study, an upregulation of TLR3 was shown in C6661 and HK1 using qRT –PCR and it was consistent with our RT-PCR result (Figure 4.1 and Figure 4.12). C6661 is a NPC cell line, positive for EBV and classified as undifferentiated carcinoma (UC) while HK1 is derived from a recurrent NPC case, EBV negative and belonging to keratinizing squamous cell carcinoma (KSCC) (Cheung et al., 1999; Huang et al., 1980). Although both cell lines had shown upregulation in TLR3 expression, it was significantly higher ($p = 0.00$) in C6661 compared to HK1. The higher expression of TLR3 in C6661 may be partly due to the presence of positive EBV infection. Previous study had indicated that Epstein–Barr virus-encoded small RNAs (EBER) can be detected by TLR3 (Li et al., 2015) and EBER may induce high expression of TLR3 in C6661 cell line. Previous studies have implicated that interaction of TLR3 with viral RNA in epithelial cells may induce overproduction of

proinflammatory cytokines leading to chronic inflammation (Abston et al., 2012; Calvén et al., 2011; Li et al., 2012). For example, interaction of rhinovirus RNA with TLR3 expressed in bronchial epithelial cells induced production of thymic stromal lymphopoietin (TSLP) (Calvén et al. 2011). The overproduction of this cytokine contributed to the development of chronic obstructive disease (COPD) which may be associated with risk of lung cancer (Calvén et al. 2011). Therefore, the association of TLR3 and EBV –associated proteins such as EBER may underlie the pathogenesis of NPC as their interaction has been implicated with prolonged chronic inflammation.

5.2 TLR4

TLR4 was found significantly ($p = 0.00$) upregulated in C6661 NPC cells compared to non-cancerous nasal epithelial cells and the tested NPC cell lines. What is unique to C6661 compared to the rest of the NPC as we know is the presence of EBV genome. There is no report on direct association between TLR4 and EBV in NPC. However, upregulated expression of TLR4 has been associated with coxsackievirus B3 (CVB3) induced viral myocarditis as silencing of TLR4 showed decreased severity of myocarditis (Zhao et al. 2015). Besides that, ectopic expression of TLR4 has been reported in numerous cancer types including lung cancer, ovarian cancer, colon cancer, breast cancer implicating its association with tumour mechanism such as inducing immunosuppressive cytokines, apoptosis resistance and production of pro-tumour cytokines (Zhou et al., 2009; Zhang et al., 2009; Kelly et al., 2006;

Mehmeti et al., 2015; He et al., 2007). In this study, we have identified possible association between TLR4 and EBV positive NPC and further investigation on the pathogenic mechanism of TLR4 in NPC would provide clues of its role in NPC.

5.3 TLR9

C6661 NPC cell line was found to have upregulated expression of TLR9 compared to non-cancerous nasal epithelial cells (NP69). This cell line which harbours the EBV was reported able to detect EBV DNA using TLR9 (Li et al., 2015; Fiola, Gosselin, et al., 2010). There was no constitutive expression of TLR9 detected in non-cancerous nasal epithelial cells (NP69) and the ectopic expression of TLR9 expression on C6661 may have been induced by the presence of EBV as significant downregulation in TLR9 expression shown in EBV-negative NPC cell lines (CNE1, CNE2, TW01, TW04, TW06, HK1, and HONE1). Additionally, Namalwa, a Burkitt lymphoma cell line which is also positive for EBV genome has been reported to have high expression of TLR9 (Henault et al., 2005). Even more, many reports have confirmed the association of TLR9 expression with cancer development such as in prostate cancer (Moreira et al. 2015), bladder cancer (Olbert et al. 2016) and oesophageal cancer (Sheyhidin et al. 2011). Overexpression of TLR9 in gastric cancer has been reported to facilitate interaction with *Helicobactor pylori*, a pathogen associated with gastric cancer

to secrete pro-tumour cytokines (Schmaußer et al, 2005). Moreira et al. (2015) reported that prostate cancer growth was promoted by TLR9-induced activation of transcriptional factors (NF- κB/RELA and STAT3). Therefore, the ectopic expression of TLR9 in NPC may play a similar pathogenic role in NPC development.

5.4 RIG I

RIG-I that belongs to the RLR family showed an interesting pattern of expression where RIG-I was upregulated in all NPC cell lines compared to NP69. RIG-I is a cytoplasmic sensor for double-stranded RNA such as EBER, Theoretically, C6661 which harbours EBV should have higher expression compared to the other EBV-negative NPC cell lines and NP69. What is intriguing is that the upregulation of RIG-I in NPC cells was reported at varying degrees regardless of the presence or absence of EBV infection. NPC cells such as CNE2 and HK1 which are EBV-negative had significantly higher expression of RIG-I compared to C6661.

We did a literature search to understand the possible role of RIG-I possible roles in tumourigenesis and found that RIG-I can also perform tumour suppressor activities (Li et al., 2014a; Li et al., 2014b). When RIG-I is unprimmed by foreign RNA, it associates with CARD domain and hel2 which allows intracellular signalling involving Src or STAT1 (Figure 5.1) which ends

up constraining tumourigenesis (Li et al., 2014a). This may explain the upregulation of RIG-I in NPC cells as an effort to constrain tumour development.

On another note, high expression of RIG-I was reported to be involved in autoimmune diseases such as rheumatoid arthritis (Imaizumi et al. 2008) by influencing inflammatory mediators such as IFN-γ and resulting in increased inflammatory reaction leading to chronic inflammation. Other reports also suggest RIG-I plays a role in activating pro-apoptotic signalling in both lung tumour and non-malignant cells (Besch et al. 2009). However, the author acknowledged that Bcl-x_L, an anti-apoptotic protein can be inhibited thus impairing RIG-I function to induce apoptosis. Thus, the expression of RIG-I may have been induced to cause apoptosis in NPC cells but anti-apoptosis mechanism in tumours may have prevented this function. Further study on the mechanism regulating RIG-I expression would provide insight into their role in NPC.

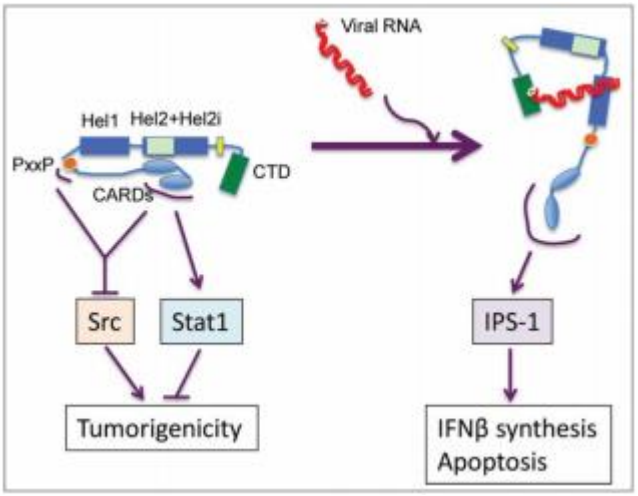

Figure 5.1: RIG-I tumour suppressor signalling. RIG-I unprimed with viral RNA associates with Src or STAT1 to constrain tumourigenesis while signalling via IPS-1 result in inflammatory response (Adopted from (Li et al., 2014a)**.**

5.5 DDX41

In our study, DDX41 was again high in all NPC cell lines compared to NP69 when further analysed using qRT –PCR, western blot and IHC. DD41 is a recently discovered DNA sensor protein that is able to sense viral dsDNA to secrete type 1 interferon (Broz & Monack 2013). The constitutive expression of DDX41 was also found in non-cancerous nasal epithelial cells (NP69). Expression of DDX41 in NP69 may indicate their important role in anti-microbial responses. Mutated DDX41 was reported to be associated with acute myeloid leukaemia through deregulation in their function and influencing signalling involved in cell proliferation leading to tumorigenesis. (Ding et al. 2012). The upregulation of expression of DDX41 in NPC cell may be an

indication of a possible role in NPC development. However, further investigation is needed to unveil the possible role of DDX41 in NPC.

5.6 NLRP3

Our data from qRT –PCR as well as protein analysis were able to confirm NLRP3 was downregulated in NPC cell lines compared to non-cancerous nasal epithelial cell (NP69). NLRP3 was constitutively expressed in NP69. The absence of NLRP3 in NPC cell lines suggest that it may have been downregulated or lost during nasal epithelial cell transformation into malignant cells. A study reported that NLRP3 was also downregulated in hepatocellular carcinoma but high in hepatic inflammatory setting suggesting that NLRP3 functions in inducing inflammatory responses (Wei et al., 2014). Thus, the impaired NLRP3 expression would make cells more prone to infection and cause chronic inflammation and eventually increase risk of developing into cancer (Niebuhr et al., 2014). The impairment of NLRP3 expression in NPC cells may provide a possible explanation for the presence of massive tumour infiltrating lymphocytes in NPC tumour and may be a possible mechanism in the pathogenesis of NPC.

5.7 The limitation of our study

In this study, we did not investigate the downstream signalling molecules involved in the regulation of PRR function, thus we were unable to deduce the relation between PRR expression with the pathogenesis of NPC. Some results such as TLR9 using end point RT-PCR have shown some non-specific bands and this could be due to existence of possible isoforms for those genes and in this study, we have not investigated the possible presence of isoforms and their relation to NPC. Although we have shown that EBV may be the key factor that triggers the upregulation of TLR3, TLR4 and TLR9 in C6661, we did not show these PRR are linked to orchestrate the pathogenesis of NPC. We also did not use actual clinical samples to verify the result from NPC cells lines.

5.8 Future study

The use of NPC cell lines in this study to screen for selected PRR has given us an idea on the expression of selected PRR in NPC. For future analysis, we should verify the results using actual clinical samples. The PRR may function normally in normal epithelial cells but their expression in NPC cells may differ as many of the downstream molecules are shared for different cell signalling processes. Further study on downstream signalling molecules and

their product of secretion will provide insight into the regulation of PRR and the mechanism involved in the pathogenesis of NPC.

CHAPTER 6

CONCLUSION

In conclusion, 11 out of 15 PRR (TLR3, TLR4, TLR6, TLR9, TLR10, MDA5, RIG-I, DDX41, LRRFIP1, NLRC4 and NLRP3) were expressed at varying levels in NPC cell lines. NPC cell line harbouring the EBV (C6661) showed high expression of TLR3, TLR4 and TLR9 compared to the rest of the tested NPC cells as well as the non-cancerous nasal epithelial cell (NP69). RIG-I and DDX41 was upregulated in all tested NPC cell lines compared to non-cancerous nasal epithelial cells. Expression of NLRP3 was either absent or downregulated in NPC cell lines compared to non-cancerous nasal epithelial cells suggesting impairment of their expression in NPC. These novel findings warrant further experiments to elucidate the mechanism of the selected PRR in the pathogenesis of NPC. Future study on microRNA targeting downstream signalling molecules would provide insights into the regulation of theses PRR in NPC.

REFERENCES

Abston, E.D. et al., 2012. Th2 regulation of viral myocarditis in mice: Different roles for TLR3 versus TRIF in progression to chronic disease. *Clinical and Developmental Immunology*, pp 1-12.

Akhter, A. et al., 2009. Caspase-7 activation by the nlrc4/ipaf inflammasome restricts legionella pneumophila infection. *PLoS Pathogens*, 5(4). pp 1-13.

Akira, S. & Takeda, K., 2004. Toll-like receptor signalling. *Nat Rev Immunol*, 4(7), pp.499–511.

Allen, I.C. et al., 2009. The NLRP3 Inflammasome Mediates In Vivo Innate Immunity to Influenza A Virus through Recognition of Viral RNA. *Immunity*, 30(4), pp.556–565.

Arakawa, R. et al., 2010. Characterization of LRRFIP1. *Biochemistry and cell biology = Biochimie et biologie cellulaire*, 88(6), pp.899–906.

Ariake, K. et al., 2016. GCF2/LRRFIP1 promotes colorectal cancer metastasis and liver invasion through integrin-dependent RhoA activation. *Cancer Letters*, 325(1), pp.99–107.

Armstrong, R.W. et al., 2000. Nasopharyngeal carcinoma in Malaysian Chinese: occupational exposures to particles, formaldehyde and heat. *International journal of epidemiology*, 29, pp.991–998.

Frech, B., Strobl, U, B., Yip, T.T.C., Lau, W.H. and Nicolaus, M.L., 1993. Characterization of the antibody response to the latent infection terminal proteins of Epstein-Barr virus in patients with nasopharyngeal carcinoma. *J Gen Virol*, (1993), pp.811–818.

Basith, S. et al., 2012. Roles of toll-like receptors in cancer: A double-edged sword for defense and offense. *Archives of Pharmacal Research*, 35(8), pp.1297–1316.

Basith, S. et al., 2011. Toll-like receptor modulators : a patent review (2006 -- 2010). *Expert Opin Ther Pat*, pp.927–944.

Bei, J.X. et al., 2010. A genome-wide association study of nasopharyngeal carcinoma identifies three new susceptibility loci. *Nat Genet*, 42(7), pp.599–603.

Besch, R. et al., 2009. Proapoptotic signaling induced by RIG-I and MDA-5 results in type I interferon-independent apoptosis in human melanoma cells. *Journal of Clinical Investigation*, 119(8), pp.2399–2411.

Blanchard, P. et al., 2015. Chemotherapy and radiotherapy in nasopharyngeal carcinoma: an update of the MAC-NPC meta-analysis. *The Lancet. Oncology*, 16(6), pp.645–655.

Bornkamm, G.W. & Hammerschmidt, W., 2001. Molecular virology of Epstein-Barr virus. *Philosophical transactions of the Royal Society of London. Series B, Biological sciences*, 356(1408), pp.437–459.

Bowie, A.G., 2012. Innate sensing of bacterial cyclic dinucleotides: more than just STING. *Nature immunology*, 13(12), pp.1137–1139.

Boyle, P. & Lewin, B., 2008. World Cancer Report 2008. *International Agency for Research on Cancer (IARC), Geneva*, pp. 1-260.

Broz, P. & Monack, D.M., 2013. Newly described pattern recognition receptors team up against intracellular pathogens. *Nature reviews. Immunology*, 13(8), pp.551–565.

Calvén, J. et al., 2011. Viral stimuli trigger exaggerated thymic stromal lymphopoietin expression by chronic obstructive pulmonary disease epithelium: Role of endosomal TLR3 and cytosolic RIG-I-like helicases. *Journal of Innate Immunity*, 4(1), pp.86–99.

Cao, S.M., Simons, M.J. & Qian, C.N., 2011. The prevalence and prevention of nasopharyngeal carcinoma in China. *Chinese Journal of Cancer*, 30(2), pp.114–119.

Cao, X., 2015. Self-regulation and cross-regulation of pattern-recognition receptor signalling in health and disease. *Nature Reviews Immunology*, 16(1), pp.35–50.

Cario, E. & Podolsky, D.K., 2000. Differential alteration in intestinal epithelial cell expression of toll-like receptor 3 (TLR3) and TLR4 in inflammatory bowel disease. *Infection and immunity*, 68(12), pp.7010–7017.

Case, C.L. & Roy, C.R., 2011. Asc modulates the function of NLRC4 in response to infection of macrophages by legionella pneumophila. *mBio*, 2(4), pp.1–9.

Chae, J.J. et al., 2011. Gain-of-Function Pyrin Mutations Induce NLRP3 Protein-Independent Interleukin-1β Activation and Severe Autoinflammation in Mice. *Immunity*, 34(5), pp.755–768.

Chan, A. T.C., Teo, P.M.L. & Johnson, P.J., 2002. Nasopharyngeal carcinoma. *Annals of Oncology*, 13(7), pp.1007–1015.

Chang, E.T. & Adami, H.O., 2006. The enigmatic epidemiology of nasopharyngeal carcinoma. *Cancer Epidemiology Biomarkers and Prevention*, 15(October), pp.1765–1777.

Cheng, J.C., Chao, K.S. & Low, D., 2001. Comparison of intensity modulated radiation therapy (IMRT) treatment techniques for nasopharyngeal carcinoma. *International journal of cancer. Journal international du cancer*, 96(2), pp.126–131.

Cheung, S.T. et al., 1999. Nasopharyngeal carcinoma cell line (C666-1) consistently harbouring Epstein-Barr virus. *International Journal of Cancer*, 83(1), pp.121–126.

Chiron, D. et al., 2009. TLR3 Ligand Induces NF- B Activation and Various Fates of Multiple Myeloma Cells Depending on IFN- Production. *The Journal of Immunology*, 182(7), pp.4471–4478.

Choubey, D. et al., 2000. Cytoplasmic localization of the interferon-inducible protein that is encoded by the AIM2 (absent in melanoma) gene from the 200-gene family. *FEBS Letters*, 474(1), pp.38–42.

Chua, M.L.K. et al., 2016. Nasopharyngeal carcinoma. *The Lancet*, 387(10022), pp.1012–1024.

CT, L. et al., 1980. Characterization of seven newly established nasopharyngeal carcinoma cell lines. *Lab Invest*, 68(6), pp. 716-727.

Devi, B.C.R. et al., 2004. High incidence of nasopharyngeal carcinoma in native people of Sarawak, Borneo Island. *Cancer Epidemiology Biomarkers and Prevention*, 13(3), pp.482–486.

Ding, L. et al., 2012. Clonal evolution in relapsed acute myeloid leukaemia revealed by whole-genome sequencing. *Nature*, 481(7382), pp.506–510.

Duan, Y. et al., 2015. Nasopharyngeal carcinoma progression is mediated by EBER-triggered inflammation via the RIG-I pathway. *Cancer Letters*, 361(1), pp.67–74.

Duan, Y. et al., 2016. Nasopharyngeal carcinoma progression is mediated by EBER-triggered inflammation via the RIG-I pathway. *Cancer Letters*, 361(1), pp.67–74.

Eiró, N. et al., 2014. Toll-like receptors 3, 4 and 9 in hepatocellular carcinoma: Relationship with clinicopathological characteristics and prognosis. *Hepatology Research*, 44(7), pp.769–778.

Fiola, S. et al., 2010. TLR9 Contributes to the Recognition of EBV by Primary Monocytes and Plasmacytoid Dendritic Cells. *The journal of immunology*, 185, pp.3620–3631.

Fleming, H.E. & Paige, C.J., 2002. Cooperation between IL-7 and the pre-B cell receptor: a key to B cell selection. *Semin Immunol*, 14(6), pp.423–430.

Franchi, L. et al., 2010. The role of IL-1β in the early tumor cell - induced angiogenic response. *J Immunol*, 227(1), pp.106–128.

Fuller-Pace, F. V., 2013. DEAD box RNA helicase functions in cancer. *RNA biology*, 10(1), pp.121–32.

Funabiki, M. et al., 2014. Autoimmune Disorders Associated with Gain of Function of the Intracellular Sensor MDA5. *Immunity*, 40(2), pp.199–212. Garc, C., 2007. Toll-like receptor 4-dependent pathways as sensors of endogenous " danger " signals. *Immunologia* , 26, pp.210–215.

Guo, Y. et al., 2010. Selection of reliable reference genes for gene expression study in nasopharyngeal carcinoma. *Acta pharmacologica Sinica*, 31(11), pp.1487–94.

He, J.-F. et al., 2007. Genetic polymorphisms of TLR3 are associated with Nasopharyngeal carcinoma risk in Cantonese population. *BMC cancer*, 7, pp.1 - 7.

He, W. et al., 2007. TLR4 signaling promotes immune escape of human lung cancer cells by inducing immunosuppressive cytokines and apoptosis resistance. *Molecular Immunology*, 44(11), pp.2850–2859.

Henault, M. et al., 2005. The human Burkitt lymphoma cell line Namalwa represents a homogenous cell system characterized by high levels of Toll-like receptor 9 and activation by CpG oligonucleotides. *Journal of Immunological Methods*, 300(1–2), pp.93–99.

Henle, G. & Henle, W., 1976. Epstein-Barr virus-specific IgA serum antibodies as an outstanding feature of nasopharyngeal carcinoma. *International journal of cancer. Journal international du cancer*, 17(1), pp.1–7.

Hu, B. et al., 2010. Inflammation-induced tumorigenesis in the colon is regulated by caspase-1 and NLRC4. *Proceedings of the National Academy of Sciences of the United States of America*, 107(50), pp.21635–21640.

Hu, L.-F. et al., 2008. A genome-wide scan suggests a susceptibility locus on 5p 13 for nasopharyngeal carcinoma. *European journal of human genetics : EJHG*, 16, pp.343–349.

Huang, D.P. et al., 1980. Establishment of a cell line (NPC/HK1) from a differentiated squamous carcinoma of the nasopharynx. *International Journal of Cancer*, 26(2), pp.127–132.

Imaizumi, T. et al., 2008. Involvement of retinoic acid-inducible gene-I in inflammation of rheumatoid fibroblast-like synoviocytes. *Clinical and Experimental Immunology*, 153(2), pp.240–244.

Iwakiri, D., 2014. Epstein-Barr Virus-Encoded RNAs: Key Molecules in Viral Pathogenesis. *Cancers*, 6(3), pp.1615–30.

Jin, T. et al., 2013. Structure of the absent in melanoma 2 (AIM2) pyrin domain provides insights into the mechanisms of AIM2 autoinhibition and inflammasome assembly. *Journal of Biological Chemistry*, 288(19), pp.13225–13235.

Jopeace, A.L. et al., 2012. Pattern recognition receptors and infectious diseases. *Intech open*, pp.383-414

Kang, M.-S. & Kieff, E., 2015. Epstein-Barr virus latent genes. *Experimental & molecular medicine*, 47(1), pp. 1- 16.

Kawai, T. & Akira, S., 2005. Pathogen recognition with Toll-like receptors. *Curr Opin Immunol* ,pp.338–344.

Kawai, T. & Akira, S., 2010. The role of pattern-recognition receptors in innate immunity: update on Toll-like receptors. *Nature immunology*, 11(5), pp.373–384.

Kawai, T. & Akira, S., 2011. Toll-like Receptors and Their Crosstalk with Other Innate Receptors in Infection and Immunity. *Immunity*, 34(5), pp.637–650.

Keating, S.E., Baran, M. & Bowie, A.G., 2016. Cytosolic DNA sensors regulating type I interferon induction. *Trends in Immunology*, 32(12), pp.574–581.

Kelly, M.G. et al., 2006. TLR-4 signaling promotes tumor growth and paclitaxel chemoresistance in ovarian cancer. *Cancer Research*, 66(7), pp.3859–3868.

Kitamura, A. et al., 2014. An inherited mutation in NLRC4 causes autoinflammation in human and mice. *Journal of Experimental Medicine*, 211(12), pp.2385–2396.

Kondo, Y. et al., 2012. Overexpression of the DNA sensor proteins, absent in melanoma 2 and interferon-inducible 16, contributes to tumorigenesis of oral squamous cell carcinoma with p53 inactivation. *Cancer Science*, 103(4), pp.782–790.

Krieg, A.M., 2006. Therapeutic potential of Toll-like receptor 9 activation. *Nature reviews. Drug discovery*, 5(6), pp.471–484.

Kuchipudi, S.V. et al., 2012. 18S rRNA is a reliable normalisation gene for real time PCR based on influenza virus infected cells. *Virology Journal*, 9(1), pp.1-7.

Kumar, H., Kawai, T. & Akira, S., 2009. Toll-like receptors and innate immunity. *Biochem.Biophys.Res.Commun.*, 388(4), pp.621–625.

Kutikhin, A.G. & Yuzhalin, A.E., 2012. C-type lectin receptors and RIG-I-like receptors: New points on the oncogenomics map. *Cancer Management and Research*, 4(1), pp.39–53.

Langereis, M.A., Feng, Q. & Frank, J.V.K., 2013. MDA5 localizes to stress granules, but this localization is not required for the induction of type I interferon. *Journal of virology*, 87(11), pp.6314–25.

Lebedev, K.A. & Ponyakina, I.D., 2006. Immunophysiology of epithelial cells and pattern-recognition receptors. *Human Physiology*, 32(2), pp.224–234.

Lee, M.S. & Kim, Y.J., 2007. Pattern-recognition receptor signaling initiated from extracellular, membrane, and cytoplasmic space. *Molecules and cells*, 23(1), pp.1–10.

Lee, S.M.Y. et al., 2014. Toll-like receptor 10 is involved in induction of innate immune responses to influenza virus infection. *Proceedings of the National Academy of Sciences of the United States of America*, 111(10), pp.3793–8.

Li, J. et al., 2007. Functional inactivation of EBV-specific T-lymphocytes in nasopharyngeal carcinoma: Implications for tumor immunotherapy. *PLoS ONE*, 2(11), pp.1–12.

Li, T.T., Ogino, S. & Qian, Z.R., 2014. Toll-like receptor signaling in colorectal cancer: carcinogenesis to cancer therapy. *World journal of gastroenterology*, 20(47), pp.17699–708.

Li, X.Y. et al., 2014. RIG-I Modulates Src-Mediated AKT Activation to Restrain Leukemic Stemness. *Molecular Cell*, 53(3), pp.407–419.

Li, X.Y., Guo, H.-Z. & Zhu, J., 2014. Tumor suppressor activity of RIG-I. *Molecular & Cellular Oncology*, 1(4), pp.1-7.

Li, Z. et al., 2015. EBV-encoded RNA via TLR3 induces inflammation in nasopharyngeal carcinoma. *Oncotarget*, 6(27), pp.24291–303.

Li, K. et al., 2012. Activation of chemokine and inflammatory cytokine response in HCV-infected hepatocytes depends on TLR3 sensing of HCV dsRNA intermediates. *Hepatology*, 100(2), pp.130–134.

Lin, C.F. et al., 2007. Expression of Toll-like receptors in cultured nasal epithelial cells. *Acta oto-laryngologica*, 127(4), pp.395–402.

Livak, K.J. & Schmittgen, T.D., 2001. Analysis of relative gene expression data using real-time quantitative PCR and the 2^(-ΔΔCT) method. *Methods (San Diego, Calif.)*, 25, pp.402–408.

Loo, Y.M. & Gale, M., 2011. Immune Signaling by RIG-I-like Receptors. *Immunity*, 34(5), pp.680–692.

Parkins, D.M., Whelan, S.L., Ferlay, J., Teppo, L. & Thomas, D.B., 1997. Cancer incidence in five continents. Volume VII. IARC Scientific Publication No. 155. lyon, IARC.

Marks, J.E., Phillips, J.L. & Menck, H.R., 1998. The national cancer data base report on the relationship of race and national origin to the histology of nasopharyngeal carcinoma. *Cancer*, 83(3), pp.582–588.

McCartney, S.A. & Colonna, M., 2009. Viral sensors: Diversity in pathogen recognition. *Immunological Reviews*, 227(1), pp.87–94.

Mehmeti, M. et al., 2015. Expression of functional toll like receptor 4 in estrogen receptor/progesterone receptor-negative breast cancer. *Breast cancer research : BCR*, 17(1), p.130.

Moreira, D. et al., 2015. TLR9 signaling through NF-κB / RELA and STAT3 promotes tumor-propagating potential of prostate cancer cells. *Oncotarget*, 6(19), pp.17302–17313.

Moumad, K. et al., 2013. Genetic polymorphisms in host innate immune sensor genes and the risk of nasopharyngeal carcinoma in North Africa. *G3 (Bethesda, Md.)*, 3(6), pp.971–7.

Neoplasia, V.E.V. et al., 1995. Undifferentiated, Nonkeratinizing, and Squamous Cell Carcinoma of the Nasopharynx. *Am J Pathol*, 146(6), pp.1355–1367.

Ng, L.K. et al., 2011. Toll-like receptor 2 is present in the microenvironment of oral squamous cell carcinoma. *British Journal of Cancer*, 104(3), pp.460–463.

Niebuhr, M. et al., 2014. Impaired NLRP3 inflammasome expression and function in atopic dermatitis due to Th2 milieu. *Allergy: European Journal of Allergy and Clinical Immunology*, 69(8), pp.1058–1067.

Niedzielska, I. et al., 2009. Toll-like receptors and the tendency of normal mucous membrane to transform to polyp or colorectal cancer. *Journal of Physiology and Pharmacology*, 60(3), pp.65–71.

Ning, J.P. et al., 1990. Consumption of salted fish and other risk factors for nasopharyngeal carcinoma (NPC) in Tianjin, a low-risk region for NPC in the People's Republic of China. *Journal of the National Cancer Institute*, 82(4), pp.291–296.

Olbert, P.J. et al., 2016. TLR4- and TLR9-dependent effects on cytokines, cell viability, and invasion in human bladder cancer cells. *Urologic Oncology: Seminars and Original Investigations*, 33(3), p.p19 - 27.

Onoguchi, K., Yoneyama, M. & Fujita, T., 2011. Retinoic acid-inducible gene-I-like receptors. *Journal of interferon & cytokine research : the official journal of the International Society for Interferon and Cytokine Research*, 31(1), pp.27–31.

Osorio, F. & Sousa, C.R.E., 2011. Myeloid C-type Lectin Receptors in Pathogen Recognition and Host Defense. *Immunity*, 34(5), pp.651–664.

Ou, S.H.I. et al., 2007. Epidemiology of nasopharyngeal carcinoma in the United States: Improved survival of Chinese patients within the keratinizing squamous cell carcinoma histology. *Annals of Oncology*, 18(1), pp.29–35.

Pandey, S. et al., 2015. Pattern Recognition Receptors in Cancer Progression and Metastasis. *Cancer growth and metastasis*, pp.25–34.

Patsos, G. et al., 2010. Restoration of absent in melanoma 2 (AIM2) induces G2/M cell cycle arrest and promotes invasion of colorectal cancer cells. *International Journal of Cancer*, 126(8), pp.1838–1849.

Ramanathan, M. et al., 2007. Sinonasal epithelial cell expression of toll-like receptor 9 is decreased in chronic rhinosinusitis with polyps. *American Journal of Rhinology*, 21(1), pp.110–116.

Ren, Z.F. et al., 2010. Effect of family history of cancers and environmental factors on risk of nasopharyngeal carcinoma in Guangdong, China. *Cancer Epidemiology*, 34(4), pp.419–424.

Ridnour, L.A. et al., 2013. Molecular Pathways: Toll-like Receptors in the Tumor Microenvironment--Poor Prognosis or New Therapeutic Opportunity. *Clinical Cancer Research*, 19(6), pp.1340–1346.

Rossi, A. et al., 1988. Adjuvant chemotherapy with vincristine, cyclophosphamide, and doxorubicin after radiotherapy in local-regional nasopharyngeal cancer: Results of a 4-year multicenter randomized study. *Journal of Clinical Oncology*, 6(9), pp.1401–1410.

Sandor, F. & Buc, M., 2005. Toll like receptor, function, and their ligand. *Folio Biol*, 3, pp.148–156.

Schmaußer, B., Andrulis, M., Endrich, S., Müller-Hermelink, H.K., et al., 2005. Toll-like receptors TLR4, TLR5 and TLR9 on gastric carcinoma cells: An implication for interaction with Helicobacter pylori. *International Journal of Medical Microbiology*, 295(3), pp.179–185.

Schmaußer, B., Andrulis, M., Endrich, S., Hermelink, H.K.M. & Eck, M., et al., 2005. Toll-like receptors TLR4, TLR5 and TLR9 on gastric carcinoma cells: An implication for interaction with Helicobacter pylori. *International Journal of Medical Microbiology*, 295(3), pp.179–185.

Schroder, K. & Tschopp, J., 2010. The Inflammasomes. *Cell*, 140(6), pp.821–832.

Seth, R.B. et al., 2005. Identification and Characterization of MAVS, A Mitochondrial Antiviral Signaling Protein that Activates NF- κB and IRF3. *Cell*, 122, pp.669–682.

Sheyhidin, I. et al., 2011. Overexpression of TLR3, TLR4, TLR7 and TLR9 in esophageal squamous cell carcinoma. *World Journal of Gastroenterology: WJG*, 17(32), pp.3745–3751.

Sizhong, Z., Xiukung, G. & Yi, Z., 1983. Cytogenetic studies on an epithelial cell line derived from poorly differentiated nasopharyngeal carcinoma. *International journal of cancer. Journal international du cancer*, 31(5), pp.587–590.

Sjöblom, T. et al., 2006. The Consensus Coding Sequences of Human Breast and Colorectal Cancers. *Science*, 314, pp.268–274.

Sutterwala, F.S. et al., 2007. Immune recognition of Pseudomonas aeruginosa mediated by the IPAF/NLRC4 inflammasome. *The Journal of experimental medicine*, 204(13), pp.3235–3245.

Takeuchi, O. & Akira, S., 2010. Pattern Recognition Receptors and Inflammation. *Cell*, 140(6), pp.805–820.

Tang, D. et al., 2012. PAMPs and DAMPs: Signal 0s that spur autophagy and immunity. *Immunological Reviews*, 249(1), pp.158–175.

Thompson, M.R. et al., 2011. Pattern recognition receptors and the innate immune response to viral infection. *Viruses*, 3(6), pp.920–940.

Tsai, C. et al., 2016. Contribution of Matrix Metallopeptidase-1 Genotypes , Smoking, Alcohol Drinking and Areca Chewing to Nasopharyngeal Carcinoma Susceptibility. *Anticancer res*, 3340, pp.3335–3340.

Tsao, S.W. et al., 2002. Establishment of two immortalized nasopharyngeal epithelial cell lines using SV40 large T and HPV16E6/E7 viral oncogenes. *Biochimica et Biophysica Acta - Molecular Cell Research*, 1590(1–3), pp.150–158.

Tschopp, J. & Schroder, K., 2010. NLRP3 inflammasome activation: The convergence of multiple signalling pathways on ROS production? *Nature reviews. Immunology*, 10(3), pp.210–215.

Tsuchiya, K. et al., 2010. Involvement of absent in melanoma 2 in inflammasome activation in macrophages infected with Listeria monocytogenes. *Journal of immunology (Baltimore, Md.: 1950)*, 185(2), pp.1186–1195.

Tye, H. et al., 2012. STAT3-Driven Upregulation of TLR2 Promotes Gastric Tumorigenesis Independent of Tumor Inflammation. *Cancer Cell*, 22(4), pp.466–478.

Vazquez, A. et al., 2014. Nasopharyngeal squamous cell carcinoma: a comparative analysis of keratinizing and nonkeratinizing subtypes. *International Forum of Allergy & Rhinology*, 4(8), pp.675–683.

Vérillaud, B. et al., 2012. Toll-like receptor 3 in Epstein-Barr virus-associated nasopharyngeal carcinomas: consistent expression and cytotoxic effects of its synthetic ligand poly(A:U) combined to a Smac-mimetic. *Infectious agents and cancer*, 7(1), pp.1-10.

Waldron, J. et al., 2016. Limitation of conventional two dimensional radiation therapy planning in nasopharyngeal carcinoma. *Radiotherapy and Oncology*, 68(2), pp.153–161.

Wang, Y. et al., 2016. Activation of NLRP3 inflammasome enhances the proliferation and migration of A549 lung cancer cells. *Oncology Reports*, 35(4), pp.2053–2064.

Wei, Q. et al., 2014. Deregulation of the NLRP3 inflammasome in hepatic parenchymal cells during liver cancer progression. *Laboratory investigation; a journal of technical methods and pathology*, 94(1), pp.52–62.

Wei, W.I. & Kwong, D.L.W., 2010. Current Management Strategy of Nasopharyngeal Carcinoma. *Clinical and Experimental Otorhinolaryngology*, 3(1), pp.1-12.

Wen, S. et al., 1997. Epstein-Barr virus (EBV) infection in salivary gland tumors: lytic EBV infection in nonmalignant epithelial cells surrounded by EBV-positive T-lymphoma cells. *Virology*, 227(2), pp.484–7.

Werts, C. et al., 2011. Nod-like receptors in intestinal homeostasis, inflammation, and cancer. *Journal of leukocyte biology*, 90(3), pp.471–482.

Wilkins, C. & Gale, M., 2010. Recognition of viruses by cytoplasmic sensors. *Current Opinion in Immunology*, 22(1), pp.41–47.

Xagorari, A. & Chlichlia, K., 2008. Toll-like receptors and viruses: induction of innate antiviral immune responses. *The open microbiology journal*, 2, pp.49–59.

Xiao, W. et al., 2015. Polymorphisms in TLR1, TLR6 and TLR10 genes and the risk of Graves' disease. *Autoimmunity*, 48(1), pp.13–18.

Xiong, W. et al., 2004. A Susceptibility Locus at Chromosome 3p21 Linked to Familial Nasopharyngeal Carcinoma A Susceptibility Locus at Chromosome 3p21 Linked to Familial Nasopharyngeal Carcinoma. *Cancer res*, pp.1972–1974.

Xu, Y. et al., 2013. Mycoplasma hyorhinis activates the NLRP3 inflammasome and promotes migration and invasion of gastric chancer cells. *PLoS ONE*, 8(11), pp.1–14.

Yang, P. et al., 2010. The cytosolic nucleic acid sensor LRRFIP1 mediates the production of type I interferon via a beta-catenin-dependent pathway. *Nature immunology*, 11(6), pp.487–494.

Yao, K. et al., 1990. Establishment and characterization of two epithelial tumor cell lines (HNE-1 and HONE-1) latently infected with Epstein-Barr virus and derived from nasopharyngeal carcinomas. *International Journal of Cancer*, 45(1), pp.83–89.

Yip, W.K. et al., 2009. Increase in tumour-infiltrating lymphocytes with regulatory T cell immunophenotypes and reduced ??-chain expression in nasopharyngeal carcinoma patients. *Clinical and Experimental Immunology*, 155(3), pp.412–422.

Young, L.S. & Rickinson, A.B., 2004. Epstein-Barr virus: 40 years on. *Nat.Rev.Cancer*, 4(10), pp.757–768.

Zainal, A.O. & Nor Saleha, I.T., 2011. National cancer registry report Malaysia cancer statistic - data and figure 2007. *Ministry of health Malaysia*, pp.1-139.

Zhang, Y. et al., 2009. TLR3 activation inhibits nasopharyngeal carcinoma metastasis via downregulation of chemokine receptor CXCR4. *Cancer biology & therapy*, 8, pp.1826–30.

Zhang, Y.B. et al., 2009. Increased expression of Toll-like receptors 4 and 9 in human lung cancer. *Molecular biology reports*, 36(6), pp.1475–1481.

Zhang, Y.L. et al., 2010. Different subsets of tumor infiltrating lymphocytes correlate with NPC progression in different ways. *Molecular Cancer*, 9, pp.1-11.

Zhao, Z. et al., 2015. Coxsackievirus B3 Induces Viral Myocarditis by Upregulating Toll Like Receptor 4 Expression. *Biochemistry*, 80(4), pp.534-543.

Zhiqiang Zhang, Bin Yuan, Musheng Bao, Ning Lu, Taeil Kim, and Y.-J.L., 2012. The helicase DDX41 senses intracellular DNA mediated by the adaptor STING in dendritic cells. *Nat Immunol*, 100(2), pp.130–134.

Zhou, M. et al., 2009. Toll-like receptor expression in normal ovary and ovarian tumors. *Cancer immunology, immunotherapy*, 58(9), pp.1375–85.

Zhou, R. et al., 2011. A role for mitochondria in NLRP3 inflammasome activation. *Nature*, 469(7329), pp.221–225.

APPENDICES

APPENDIX A

Table for PRR primer sequence

Gene of interest	Primer sequence	
	Forward	**Reverse**
TLR3	5’ – AGCCTTCAACGACTGATGC – 3’	5’ – TTCCAGAGCCGTGCTAAGT – 3’
TLR4	5’ – TGGACAATTTGGGCTAGAGG – 3’	5’ – ATCCCAGCCATCTGTGTCTC – 3’
TLR6	5’ – AGTAGCTGGGCTTGCATTGT – 3’	5’ – TTATTGGAGGGCCTTGAGTG – 3’
TLR7	5’ – GACCTCAGCCACAACCAACT – 3’	5’ – GGACATTTTCTGGGAAGCTG – 3’
TLR8	5’ – CCCCAAATACCCTCTGGTTT – 3’	5’ – CCAAATTTGTCAGCGTTTCA – 3’
TLR9	5’ – AAGGGGTGAAGGAGCTGTCT – 3’	5’ – ACAGCAGCTACAGGGAAGGA – 3’
TLR10	5’ – GGCCAGAAACTGTGGTCAAT – 3’	5’ – CTGCATCCAGGGAGATCAGT – 3’
MDA5	5’ – GGAACATGCAGGCAGTTGAA – 3’	5’ – CAAACGATGGAGAGGGCAAG – 3’
RIG-I	5’ – AGAGCACTTGTGGACGCTTT – 3’	5’ – TGCCTTCATCAGCAACTGAG – 3’
DDX41	5’ – GCCCTTGTAAAGCCTGTGAC – 3’	5’ – TTGAGCAGCAGGTACTCGTG – 3’
LRRFIP1	5’ – CGGCAGCAGAAGGAGATCTA – 3’	5’ – TTCCACGACTACCCACTGAC – 3’

Table continues for PRR primer sequences continued

ZDBP-1	5’ – AAGCACTGGGAATGAGGACA – 3’	5’ – TCTGGATGGCTTCGGAGTTT – 3’
Aim2	5’ – GCTGCACCAAAATCTCTCC – 3’	5’ – ACATCCTGCTTGCCTTCT – 3’
NLRC4	5’ – CTGCATCATTGAAGGGGAAT – 3’	5’ – TGTCTGCTTCCTGATTGTGC – 3’
NLRP3	5’ – CTTCTCTGATGAGGCCCAAG – 3’	5’ – GCAGCAAACTGGAAAGGAAG – 3’

APPENDIX B

Sample for calculation of fold change using excel for quantitative real time-PCR.

		TLR4							
		CNE1	CNE2	TW01	TW04	TW06	HONE1	HK1	C6661
13	Average of TLR4 expression in NPC Exp 1(A)	28.22	28.99	30.45	28.64	26.78	25.69	25.26	23.08
14	Average of TLR4 expression in NPC Exp 2 (B)	28.27	26.96	30.63	28.6	25.38	25.37	25.26	23.65
15									
16	Average CT(NPC) -CT(HKG) Exp 1	11.74	10.18	14.21	12.47	10.90	9.07	6.22	1.63
17	Average CT(NPC) -CT(HKG) Exp 2	11.70	8.79	14.42	12.00	9.65	8.78	5.74	2.02
18	Mean for both exp (E)	11.72	9.48	14.31	12.24	10.27	8.92	5.98	1.82
19									
20	Average of TLR 4 expression NP69 in Exp 1(C	28.24	28.24	28.24	28.24	28.24	28.24	28.24	28.24
21	Average of TLR 4 expression NP69 in Exp 2 (D	27.80	27.80	27.80	27.80	27.80	27.80	27.80	27.80
22	Average for HKG Exp1 (NP69)	18.65	18.65	18.65	18.65	18.65	18.65	18.65	18.65
23	Average for HKG Exp2 (NP69)	18.93	18.93	18.93	18.93	18.93	18.93	18.93	18.93
24	Average CT(NP69) -CT(HKG) Exp1	9.59	9.59	9.59	9.59	9.59	9.59	9.59	9.59
25	Average CT(NP69) -CT(HKG) Exp2	8.87	8.87	8.87	8.87	8.87	8.87	8.87	8.87
26	Mean for both exp (F)	9.23	9.23	9.23	9.23	9.23	9.23	9.23	9.23
27									
28	(A) - (C)	2.15	0.58	4.62	2.88	1.31	-0.52	-3.38	-7.96
29	(B) - (D)	2.83	-0.08	5.55	3.13	0.77	-0.09	-3.13	-6.86
30	- [(A) - (C)]	-2.15	-0.58	-4.62	-2.88	-1.31	0.52	3.38	7.96
31	- [(B) - (D)]	-2.83	0.08	-5.55	-3.13	-0.77	0.09	3.13	6.86
32	Fold change exp 1	0.23	0.67	0.04	0.14	0.40	1.44	10.37	249.00
33	Fold change exp 2	0.14	1.06	0.02	0.11	0.58	1.07	8.75	115.76
34	Negative fold change exp 1	-4.44	-1.50	-24.50	-7.36	-2.48	-0.69	-0.10	0.00
35	Negative fold change exp 2	-7.09	-0.95	-46.85	-8.75	-1.71	-0.94	-0.11	-0.01
36									
37	(E) - (F)	2.49	0.25	5.08	3.01	1.04	-0.31	-3.25	-7.41
38	Negative (E) - (F)	-2.49	-0.25	-5.08	-3.01	-1.04	0.31	3.25	7.41
39	Fold change exp 1+ exp 2	0.18	0.84	0.03	0.12	0.49	1.24	9.53	169.78
40	Negative Fold change exp 1+ exp 2	-5.61	-1.19	-33.88	-8.03	-2.06	-0.81	-0.10	-0.01
41	Fold change values for graph plotting	1.20	-1.19	-33.88	-8.03	-2.06	1.24	1.41	169.78
42	Standard error	0.05	0.22	0.01	0.01	0.1	0.21	0.93	28.2

APPENDIX C

Sample output for statistical analysis using 1 way anova in the calculation of significant difference in TLR4 expression between NPC cell lines and non-cancerous nasal epithelial cells.

Post Hoc Tests

Multiple Comparisons

TLR4

LSD

(I) NPC_cell_line	(J) NPC_cell_line	Mean Difference (I-J)	Std. Error	Sig.	95% Confidence Interval	
					Lower Bound	Upper Bound
CNE1	CNE2	-6.90333	5.23557	.194	-17.4483	3.6417
	TW01	28.89667*	5.23557	.000	18.3517	39.4417
	TW04	2.18000	5.23557	.679	-8.3650	12.7250
	TW06	-3.62333	5.23557	.492	-14.1683	6.9217
	HONE1	-7.42000	5.23557	.163	-17.9650	3.1250
	HK1	-15.93333*	5.23557	.004	-26.4783	-5.3883
	C6661	-238.77000*	5.23557	.000	-249.3150	-228.2250
	NP69	-7.10333	5.23557	.182	-17.6483	3.4417
CNE2	CNE1	6.90333	5.23557	.194	-3.6417	17.4483
	TW01	35.80000*	5.23557	.000	25.2550	46.3450
	TW04	9.08333	5.23557	.090	-1.4617	19.6283
	TW06	3.28000	5.23557	.534	-7.2650	13.8250
	HONE1	-.51667	5.23557	.922	-11.0617	10.0283
	HK1	-9.03000	5.23557	.091	-19.5750	1.5150
	C6661	-231.86667*	5.23557	.000	-242.4117	-221.3217
	NP69	-.20000	5.23557	.970	-10.7450	10.3450
TW01	CNE1	-28.89667*	5.23557	.000	-39.4417	-18.3517
	CNE2	-35.80000*	5.23557	.000	-46.3450	-25.2550

	TW04	-26.71667*	5.23557	.000	-37.2617	-16.1717
	TW06	-32.52000*	5.23557	.000	-43.0650	-21.9750
	HONE1	-36.31667*	5.23557	.000	-46.8617	-25.7717
	HK1	-44.83000*	5.23557	.000	-55.3750	-34.2850
	C6661	-267.66667*	5.23557	.000	-278.2117	-257.1217
	NP69	-36.00000*	5.23557	.000	-46.5450	-25.4550
TW04	CNE1	-2.18000	5.23557	.679	-12.7250	8.3650
	CNE2	-9.08333	5.23557	.090	-19.6283	1.4617
	TW01	26.71667*	5.23557	.000	16.1717	37.2617
	TW06	-5.80333	5.23557	.274	-16.3483	4.7417
	HONE1	-9.60000	5.23557	.073	-20.1450	.9450
	HK1	-18.11333*	5.23557	.001	-28.6583	-7.5683
	C6661	-240.95000*	5.23557	.000	-251.4950	-230.4050
	NP69	-9.28333	5.23557	.083	-19.8283	1.2617
TW06	CNE1	3.62333	5.23557	.492	-6.9217	14.1683
	CNE2	-3.28000	5.23557	.534	-13.8250	7.2650
	TW01	32.52000*	5.23557	.000	21.9750	43.0650
	TW04	5.80333	5.23557	.274	-4.7417	16.3483
	HONE1	-3.79667	5.23557	.472	-14.3417	6.7483
	HK1	-12.31000*	5.23557	.023	-22.8550	-1.7650
	C6661	-235.14667*	5.23557	.000	-245.6917	-224.6017
	NP69	-3.48000	5.23557	.510	-14.0250	7.0650
HONE1	CNE1	7.42000	5.23557	.163	-3.1250	17.9650
	CNE2	.51667	5.23557	.922	-10.0283	11.0617
	TW01	36.31667*	5.23557	.000	25.7717	46.8617
	TW04	9.60000	5.23557	.073	-.9450	20.1450
	TW06	3.79667	5.23557	.472	-6.7483	14.3417
	HK1	-8.51333	5.23557	.111	-19.0583	2.0317
	C6661	-231.35000*	5.23557	.000	-241.8950	-220.8050
	NP69	.31667	5.23557	.952	-10.2283	10.8617
HK1	CNE1	15.93333*	5.23557	.004	5.3883	26.4783
	CNE2	9.03000	5.23557	.091	-1.5150	19.5750
	TW01	44.83000*	5.23557	.000	34.2850	55.3750

	TW04	18.11333*	5.23557	.001	7.5683	28.6583
	TW06	12.31000*	5.23557	.023	1.7650	22.8550
	HONE1	8.51333	5.23557	.111	-2.0317	19.0583
	C6661	-222.83667*	5.23557	.000	-233.3817	-212.2917
	NP69	8.83000	5.23557	.099	-1.7150	19.3750
C6661	CNE1	238.77000*	5.23557	.000	228.2250	249.3150
	CNE2	231.86667*	5.23557	.000	221.3217	242.4117
	TW01	267.66667*	5.23557	.000	257.1217	278.2117
	TW04	240.95000*	5.23557	.000	230.4050	251.4950
	TW06	235.14667*	5.23557	.000	224.6017	245.6917
	HONE1	231.35000*	5.23557	.000	220.8050	241.8950
	HK1	222.83667*	5.23557	.000	212.2917	233.3817
	NP69	231.66667*	5.23557	.000	221.1217	242.2117
NP69	CNE1	7.10333	5.23557	.182	-3.4417	17.6483
	CNE2	.20000	5.23557	.970	-10.3450	10.7450
	TW01	36.00000*	5.23557	.000	25.4550	46.5450
	TW04	9.28333	5.23557	.083	-1.2617	19.8283
	TW06	3.48000	5.23557	.510	-7.0650	14.0250
	HONE1	-.31667	5.23557	.952	-10.8617	10.2283
	HK1	-8.83000	5.23557	.099	-19.3750	1.7150
	C6661	-231.66667*	5.23557	.000	-242.2117	-221.1217

*. The mean difference is significant at the 0.05 level.